

# **Becker & Hickl GmbH**

**DCS-120**

**Confocal Scanning FLIM Systems**

**An Overview**

**2015**





## DCS-120 FLIM System

Becker & Hickl GmbH  
Nahmitzer Damm 30  
12277 Berlin  
Germany  
Tel. +49 / 30 / 787 56 32  
FAX +49 / 30 / 787 57 34  
<http://www.becker-hickl.com>  
email: [info@becker-hickl.com](mailto:info@becker-hickl.com)

April 2015

This brochure is subject to copyright. However, reproduction of small portions of the material in scientific papers or other non-commercial publications is considered fair use under the copyright law. It is requested that a complete citation be included in the publication. If you require confirmation please feel free to contact Becker & Hickl.

# The DCS-120 Confocal Scanning FLIM System

## An Overview

*Abstract:* The DCS-120 system uses excitation by ps diode lasers or femtosecond titanium-sapphire lasers, fast scanning by galvanometer mirrors, confocal detection, and FLIM by bh's multidimensional TCSPC technique to record fluorescence lifetime images at high temporal resolution, high spatial resolution, and high sensitivity [3]. The DCS-120 system is available with inverted microscopes of Nikon, Zeiss, and Olympus. It can also be used to convert an existing conventional microscope into a fully functional confocal or multiphoton laser scanning microscope with TCSPC detection. Due to its fast beam scanning and its high sensitivity the DCS-120 system is compatible with live-cell imaging. DCS-120 functions include simultaneous recording of FLIM or steady-state fluorescence images simultaneously in two fully parallel wavelength channels, laser wavelength multiplexing, time-series FLIM, time-series recording, Z stack FLIM, phosphorescence lifetime imaging (PLIM), fluorescence lifetime-transient scanning (FLITS) and FCS recording. Applications focus on lifetime variations by interactions of fluorophores with their molecular environment. Typical applications are ion concentration measurement, FRET experiments, autofluorescence imaging, and plant physiology.

### Introduction

The DCS-120 systems are complete confocal laser scanning microscopes for fluorescence lifetime imaging. The systems use bh's multi-dimensional TCSPC FLIM technology [15, 21, 23] in combination with fast laser scanning and confocal detection [24]. DCS-120 systems are available with various inverted and upright microscopes, see Fig. 1. The DCS-120 scan head with the control and data acquisition electronics can also be used to upgrade a conventional microscope with FLIM recording. A 'DCS-120 MACRO' system is available for FLIM of centimetre-size objects, see Fig. 2.

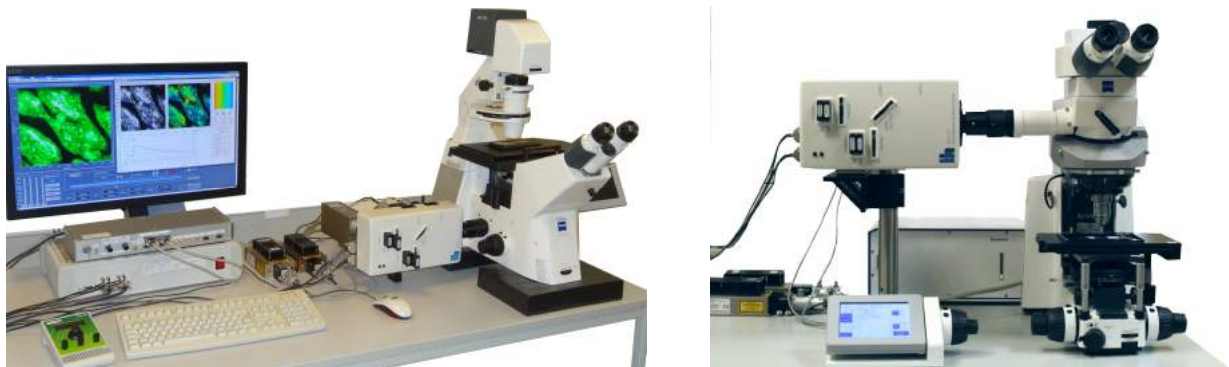


Fig. 1: The DCS-120 system with a Zeiss Axio Observer microscope (left) and Zeiss Axio Examiner (right) .

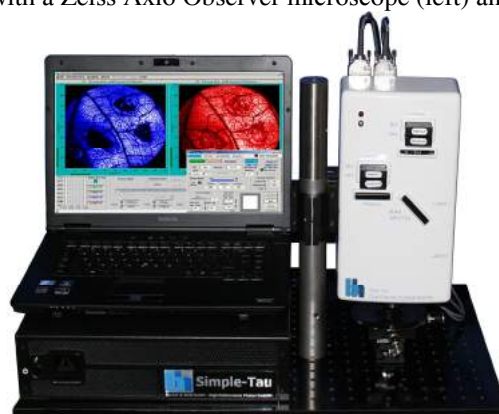


Fig. 2: DCS-120 MACRO system

In the basic configuration, the DCS-120 uses excitation by two ps diode lasers and records in two fully parallel detector and TCSPC channels. The systems are using highly efficient GaAsP hybrid detectors. By combining extremely high efficiency with large active area, high counting speed, high time-resolution, and low background, these detectors have initiated a breakthrough in FLIM recording [21]. Another step was made by the introduction of 64-bit data acquisition software [9, 40]. FLIM data are now recorded at unprecedented pixel numbers, high dynamic range, short acquisition time, and minimum exposure of the sample. New hardware and software functions have resulted in advanced FLIM functions, like time-series FLIM, Z stack FLIM, temporal Mosaic FLIM, wavelength-multiplexed FLIM, combined fluorescence and phosphorescence lifetime imaging (FLIM/PLIM), and fluorescence lifetime-transient scanning (FLITS). Due to its high sensitivity, the system can also be used for FCS recording and single-molecule spectroscopy. 16-channel multi-wavelength FLIM is available as an option. It uses a new multi-wavelength detector with a GaAsP cathode. Due to the high efficiency of the detector and the large memory space available in the 64 bit environment multi-wavelength FLIM can be recorded with unprecedented pixel numbers [9, 40]. Advanced versions of the DCS-120 system are available for multiphoton excitation and tuneable excitation sources [6, 7].

## Principle

### Multi-Dimensional TCSPC

The bh FLIM systems use a combination of bh's multidimensional time-correlated single-photon counting process with confocal or multiphoton laser scanning. The sample is continuously scanned by a high-repetition rate pulsed laser beam, single photons of the fluorescence signal are detected, and each photon is characterised by its time in the laser pulse period and the coordinates of the laser spot in the scanning area in the moment of its detection. The recording process builds up a photon distribution over these parameters, see Fig. 3. The photon distribution can be interpreted as an array of pixels, each containing a full fluorescence decay curve in a large number of time channels.

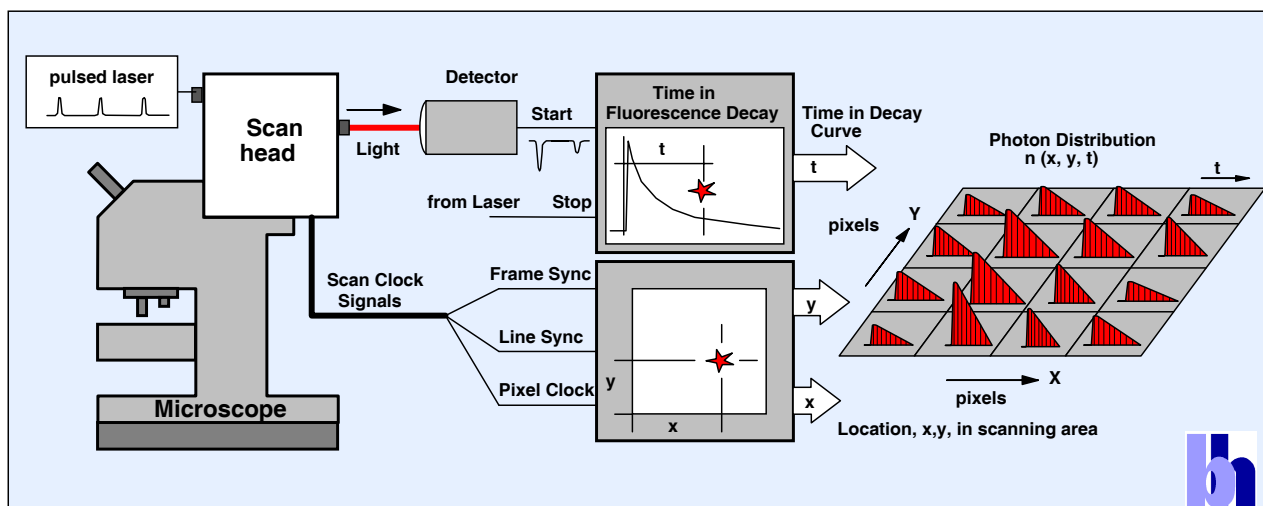


Fig. 3: Principle of TCSPC FLIM

The recording process delivers a near-ideal photon efficiency, excellent time resolution, and is independent of the speed of the scanner. The signal-to-noise ratio depends only on the total acquisition time and the photon rate available from the sample.

The technique can be extended by including additional parameters in the photon distribution. These can be the depth of the focus in the sample, the wavelength of the photons, the time after a stimulation of the sample, or the time within the period of an additional modulation of the laser. These techniques are used to record Z stacks or mosaics of FLIM images, multi-wavelength FLIM images, images of physiological effects occurring in the sample, or to record simultaneously fluorescence and phosphorescence lifetime images.

### *Confocal Scanning*

The DCS-120 scan head contains the complete beam deflection and confocal detection optics. A simplified optical diagram is shown in Fig. 4. The laser beams are deflected by fast-moving galvanometer mirrors, and sent down the microscope beam path. The axis of the galvanometer mirrors is projected into the plane of the microscope lens. With the motion of the galvanometer mirrors the laser focus thus scans over the focal plane in the sample. The emission light is collected back through the microscope lens. The beam is descanned by the galvanometer mirrors, separated from the excitation beam, split into two channels of different wavelength or different polarisation and focused into pinholes in a plane conjugate with the focal plane in the sample. Out-of-focus light is not focused into the pinholes and thus suppressed. Please see [3] for details of the optical system.

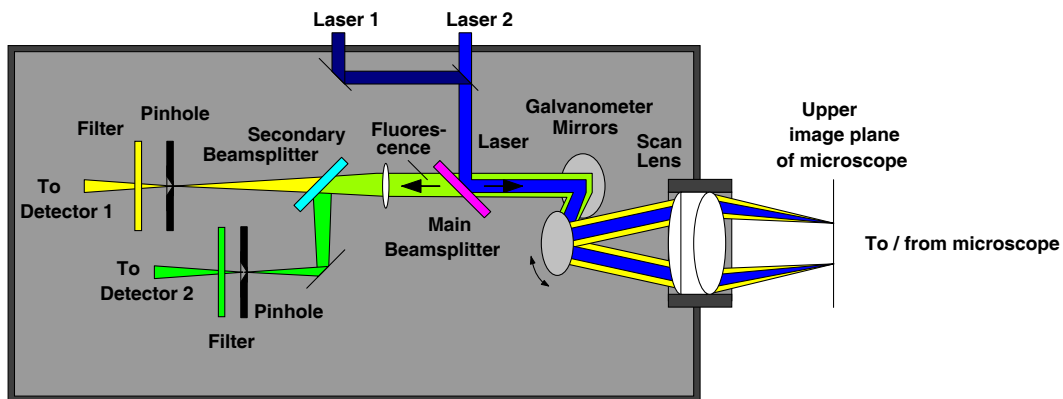


Fig. 4: Optical diagram of the DCS-120 scan head. Simplified, see [3] for details

The DCS-120 system is highly modular. The DCS-120 scan head is compatible with conventional microscopes of almost any type and manufacturer. Complete laser scanning systems are available with microscopes of Zeiss, Nikon, and Olympus. The DCS-120 MACRO system scans macroscopic objects directly in the image plane of the scan head. The DCS system can be used with a variety of different lasers and detectors. It can be operated with ps diode lasers of various wavelength, with tuneable excitation sources, and with fs lasers for multiphoton excitation.



## DCS-120 Functions in Brief

### 64-bit SPCM Data Acquisition Software

The DCS-120 FLIM systems use the bh SPCM data acquisition software. Since 2013 the SPCM software is available in a 64-bit version. SPCM 64 bit exploits the full capability of Windows 64 bit, resulting in faster data processing, capability of recording images of extremely large pixel numbers, and availability of additional multi-dimensional FLIM modes [9, 21, 40]. The main panel of the SPCM data acquisition software is configurable by the user [21]. Different configurations for FLIM systems are shown in Fig. 5.

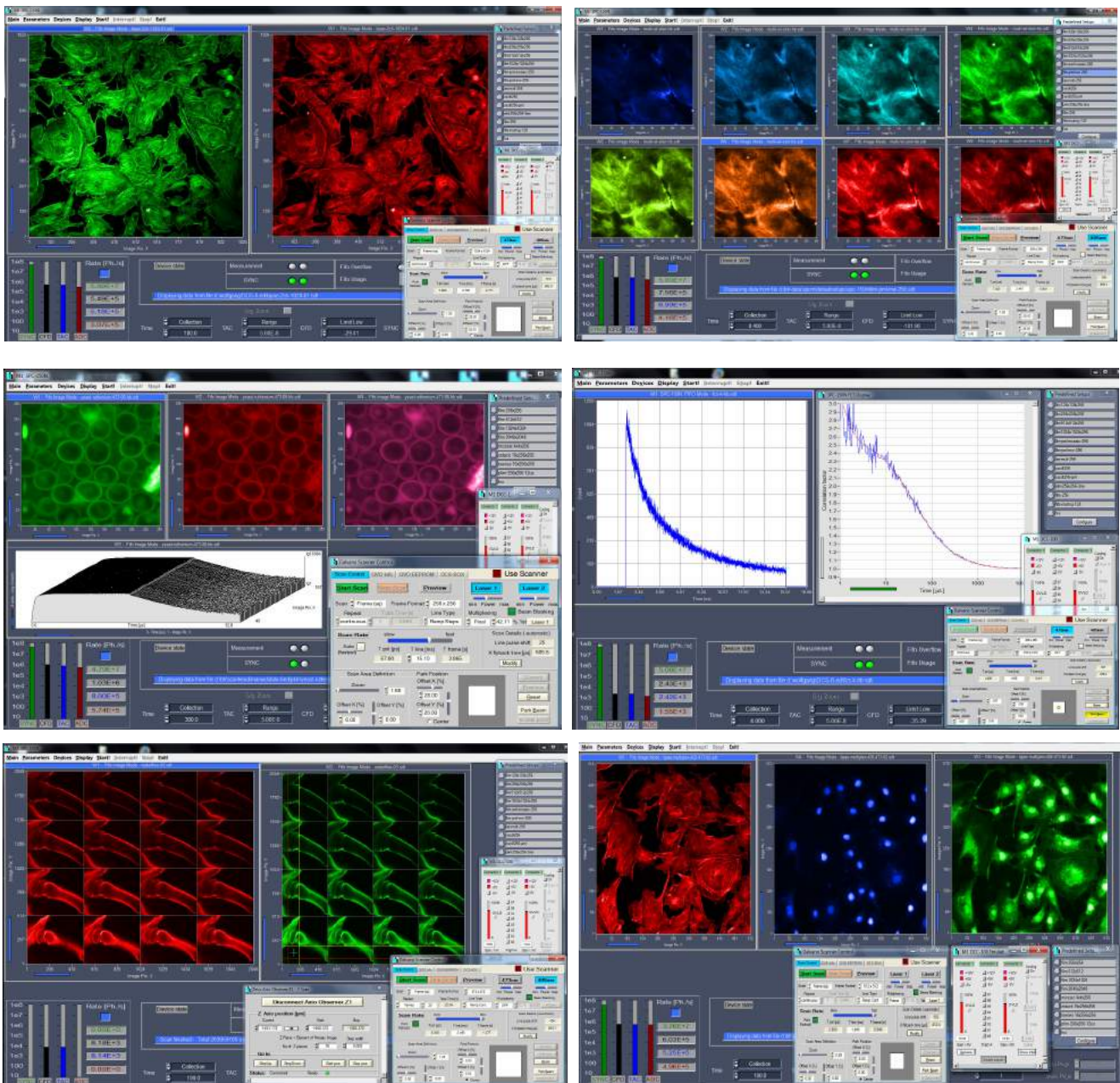


Fig. 5: SPCM software panel. Top left to bottom right: FLIM with two detector channels, multi-spectral FLIM, combined fluorescence / phosphorescence lifetime imaging (FLIM/PLIM), fluorescence correlation (FCS), Z-Stack FLIM, Excitation-wavelength multiplexed FLIM

### *Easy Change Between Instrument Configurations*

Frequently used instrument configurations are stored in a 'Predefined Setup' panel. Changing between the different configurations and user interfaces is just a matter of a single mouse click, see Fig. 6.

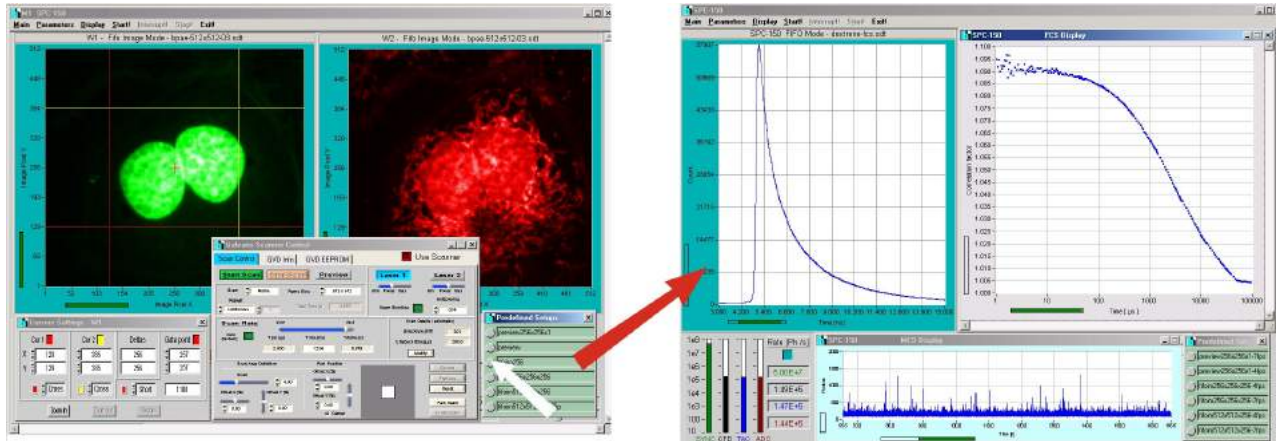


Fig. 6: Changing between different instrument configurations: The DCS-120 system switches from a FLIM configuration into an FCS configuration by a simple mouse click

### *Interactive Scanner Control*

The scanner control is fully integrated in the SPCM data acquisition software. The zoom factor and the position of the scan area can be adjusted via the scanner control panel or via the cursors of the display window. Changes in the scan parameters are executed online, without stopping the scan. Whatever you change in the microscope: The position of the samples, the scan area, the zoom factor, the focal plane, pinhole size or the laser power - the result becomes immediately visible in the preview images.

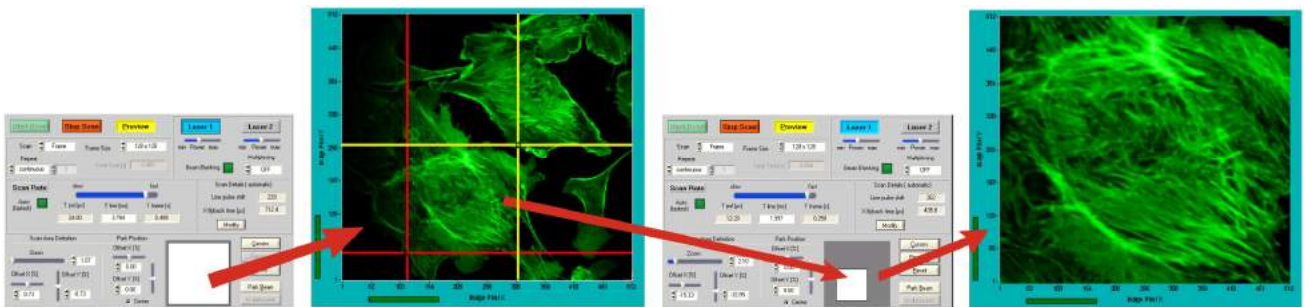


Fig. 7: Interactive scanner control

### *Automatic Scanner Speed*

Depending on the frame format and the zoom factor, the DCS-120 scanner control automatically selects the maximum speed of the scanner. The scanner thus always runs at high pixel rate, resulting in fast acquisition, minimum triplet excitation, and minimum photobleaching.

### *Fast preview function*

When FLIM is applied to live samples the time and exposure needed for sample positioning, focusing, laser power adjustment, and region-of-interest selection has to be minimised. Therefore, the FLIM systems have a fast preview function. The preview function displays images in intervals on the order of 1 second and less, see Fig. 8.



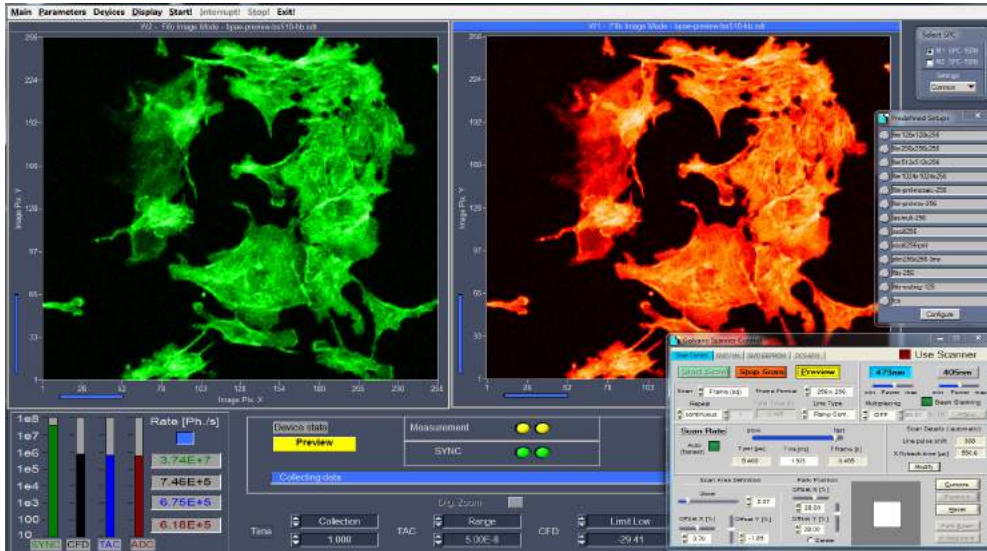


Fig. 8: SPCM software in fast preview mode, display rate one image per second.

## Fast Beam Scanning - Fast Acquisition

The DCS-120 uses fast beam scanning by galvanometer mirrors. A complete frame is scanned within a time from 100 ms to a few seconds, with pixel dwell times down to one microsecond.

Compared with sample scanning, beam scanning is not only much faster, it avoids also induction of cell motion by exerting dynamic forces on the sample. Moreover, live cell imaging requires a fast preview function for fluorescence images for sample positioning and focusing. This can only be provided if the beam is scanned at a high frame rate. With its fast scanner and its multi-dimensional TCSPC process the DCS system achieves surprisingly short acquisition times, see Fig. 9.

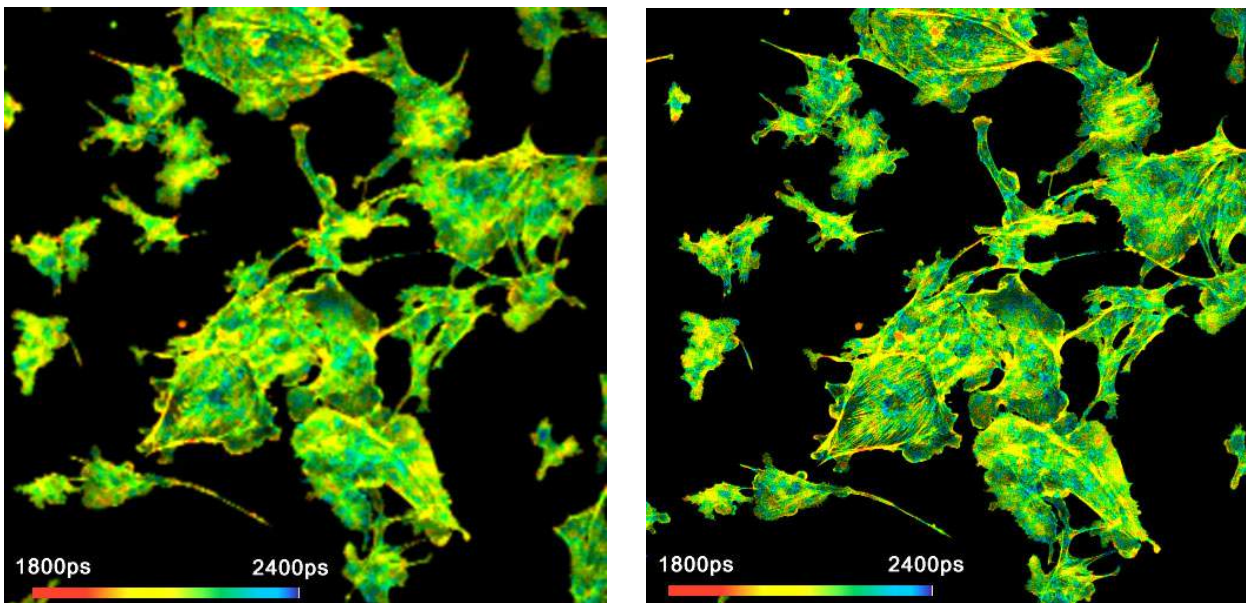


Fig. 9: FLIM images recorded within 5 seconds acquisition time. 256 x 256 pixels (left) and 512 x 512 pixels (right), both with 256 time channels.

Fast scanning is also the basis of recording fast FLIM time series. With the DCS-120 time-series can be recorded as fast as two images per second [34]. An example is shown in Fig. 10.



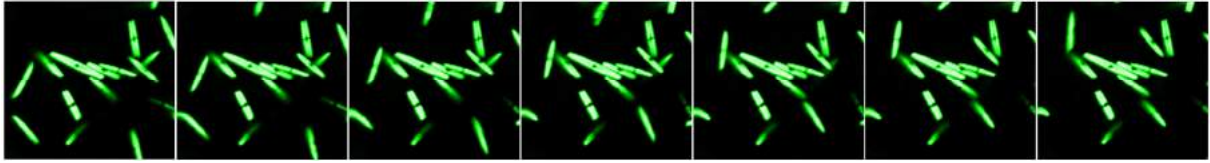


Fig. 10: Bacteria in motion. Autofluorescence, acquisition speed 2 images per second, scan speed 6 frames per second

### ***High-Efficiency GaAsP Hybrid Detectors***

The new bh HPM-100-40 GaAsP hybrid detectors of the DCS-120 combine SPAD-like sensitivity with the large active area of a PMT [4]. The large area avoids any alignment problems, and allows light to be efficiently collected through large pinholes, see Fig. 11, and from the non-descanned beam path of multiphoton microscopes [17]. In contrast to SPADs, there is no ‘diffusion tail’ in the temporal response. Moreover, the hybrid detectors are free of afterpulsing. The absence of afterpulsing results in improved contrast, higher dynamic range of the decay curves recorded, and in the capability to obtain FCS data from a single detector.

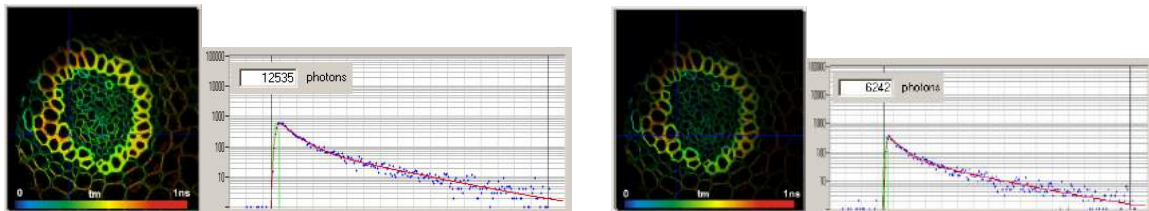


Fig. 11: Fluorescence lifetime images recorded with an HPM-100-40 hybrid detector (left) and with an id-100-50 SPAD (right). Images and decay functions at selected cursor position.

### ***Detection in Two Fully Parallel Channels***

With its two detection channels the DCS-120 system records in two wavelength intervals simultaneously. The signals are detected by separate detectors and processed by separate TCSPC modules. There is no intensity or lifetime crosstalk due to counting loss or pile up [15, 21]. Even if one channel overloads the other one is still able to produce correct data.

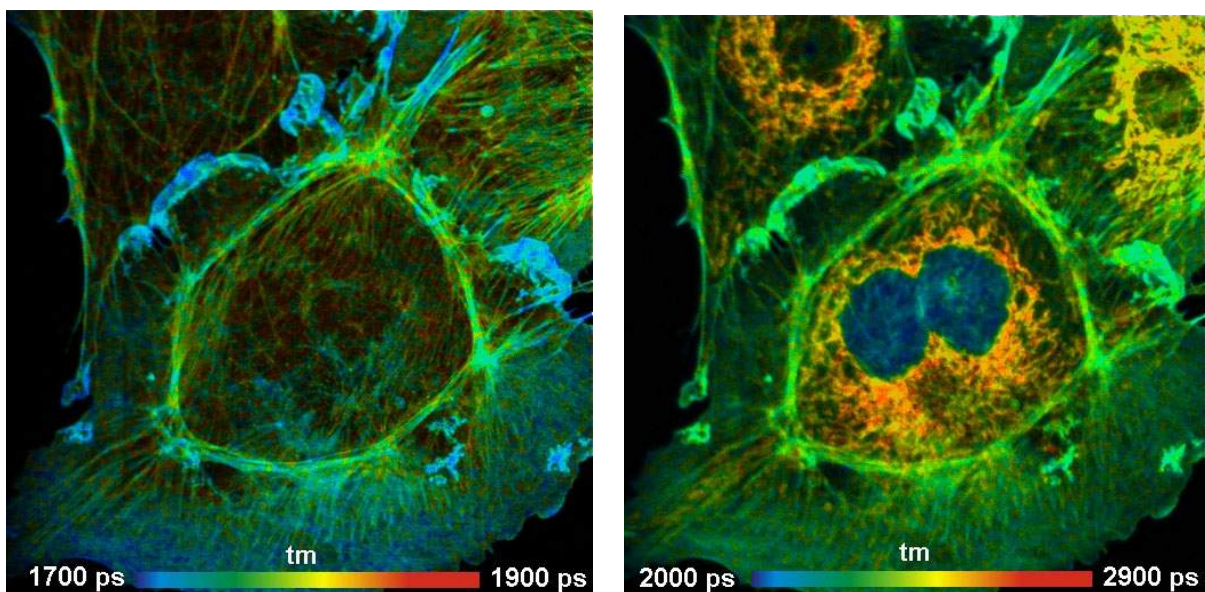


Fig. 12: Dual-wavelength detection. BPAE cells stained with Alexa 488 phalloidin and Mito Tracker Red. Left: 484 nm to 560 nm. Right: 590 nm to 650 nm.



### Megapixel FLIM Images

With 64 bit SPCM software pixel numbers can be increased to 2048 x 2048 pixels, with a temporal resolution of 256 time channels. Two such images are recorded simultaneously in different wavelength channels. Fig. 13 and Fig. 14 (facing page) show an example.

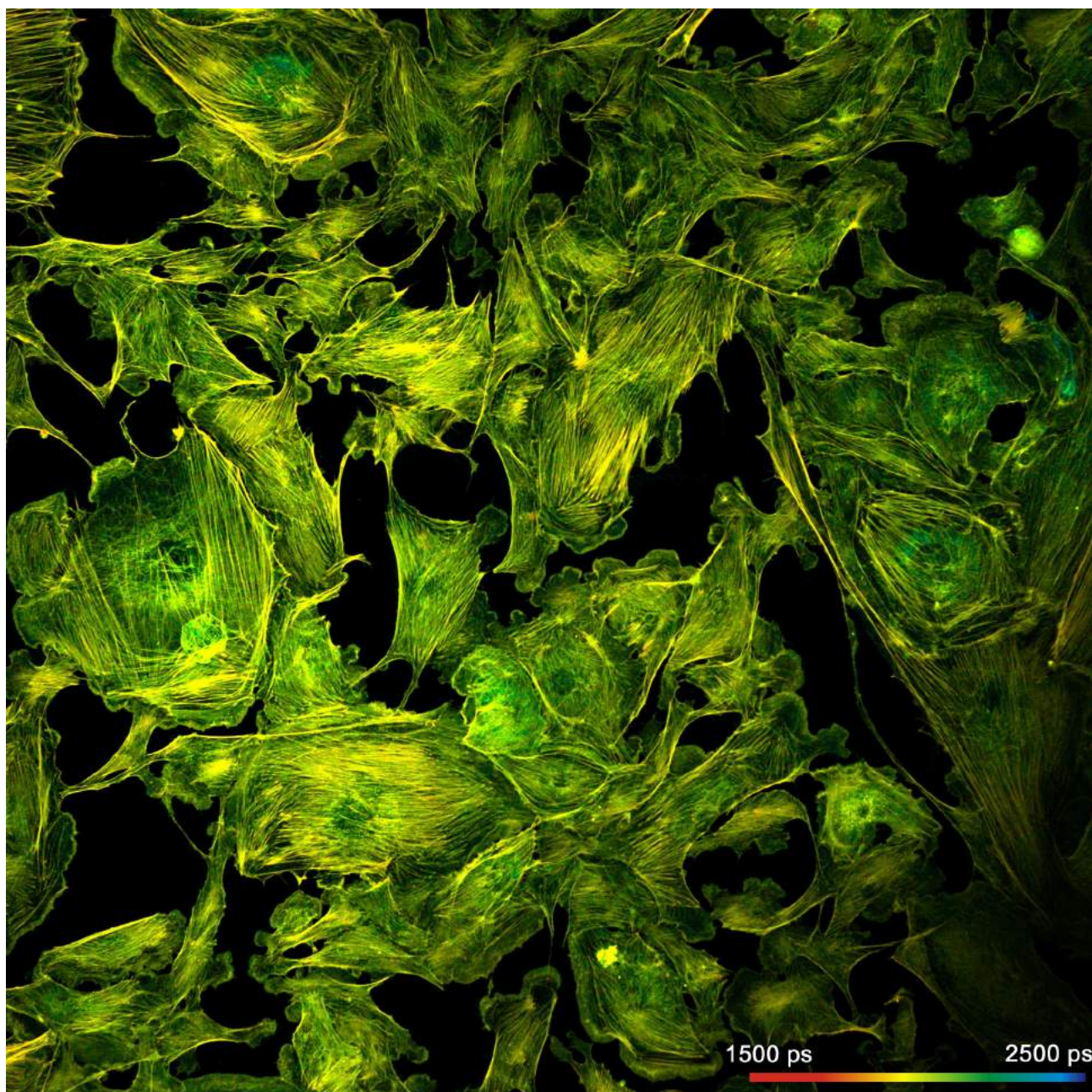


Fig. 13: BPAE sample (Invitrogen) scanned with 2048 x 2048 pixels. Green channel, 485 to 560 nm

The large pixel numbers available in SPCM 64 bit allow the full field of view of even the best microscope lenses to be scanned with an oversampling factor of two or more. In other words, extremely large image areas can be scanned without without compromising spatial resolution.



Large pixel numbers are especially important for tissue imaging. They are also useful in cases when a large number of cells have to be investigated and the FLIM results to be compared. Megapixel FLIM records images of many cells simultaneously, and under identical environment conditions. Moreover, the data are analysed in a single analysis run, with identical IRFs and fit parameters. The results are therefore exactly comparable for all cells in the image area.

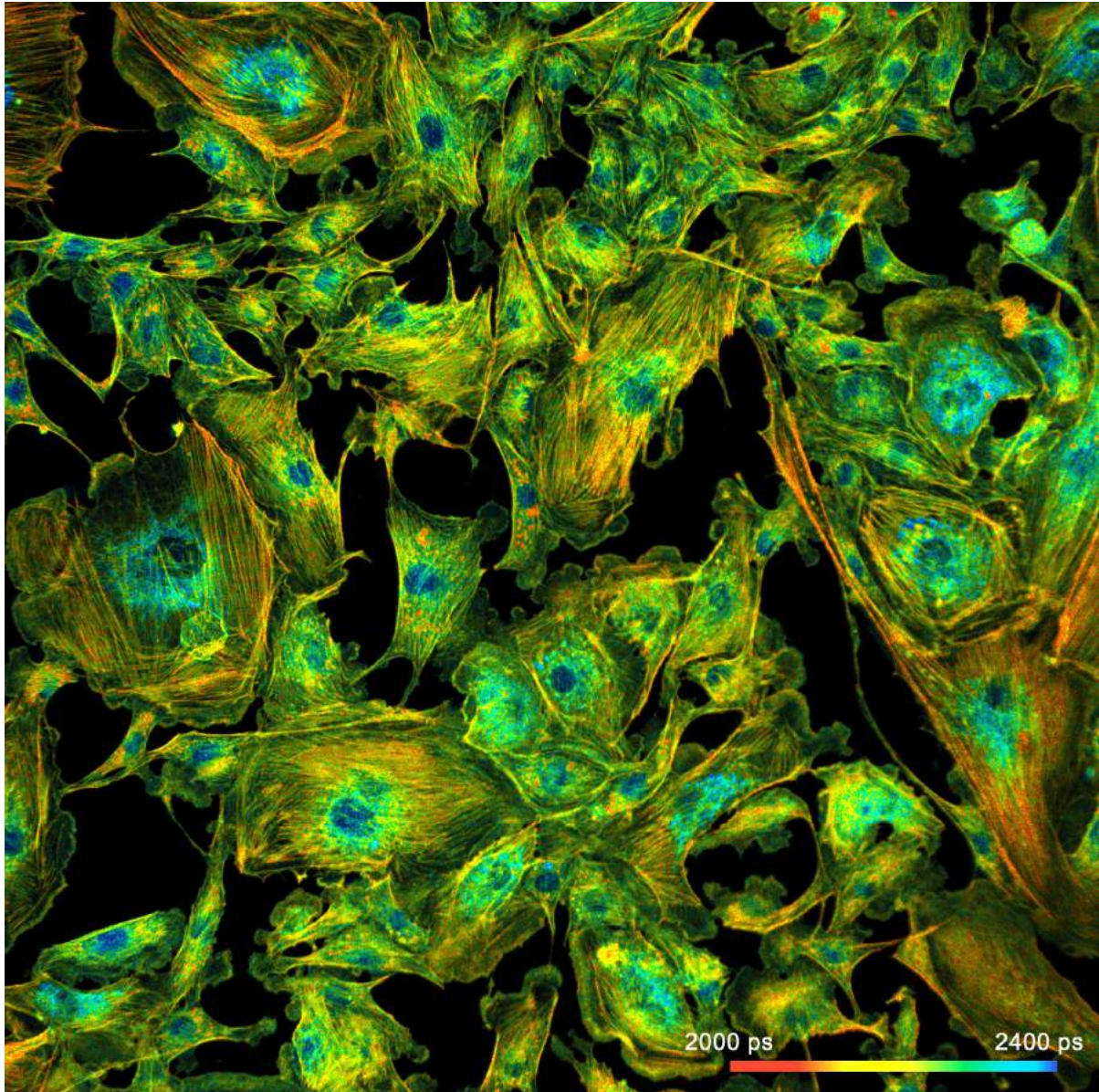


Fig. 14: BPAE sample (Invitrogen), scanned with 2048 x 2048 pixels. Red channel, 560 to 650 nm

### Multi-Wavelength FLIM

With the bh multispectral FLIM detectors the DCS-120 records FLIM simultaneously in 16 wavelength channels [13, 16, 21]. The images are recorded by a multi-dimensional TCSPC process which uses the wavelength of the photons as a coordinate of the photon distribution. There is no time gating, no wavelength scanning and, consequently, no loss of photons in this process. The system thus reaches near-ideal recording efficiency. Moreover, dynamic effects in the sample or photobleaching do not cause distortions in the spectra or decay functions. Multi-wavelength FLIM got an additional push



from the new 64-bit SPCM software, and from the introduction of a highly efficient GaAsP multi-wavelength detector. 64-bit software works with enormously large photon distributions, and the GaAsP detector delivers the efficiency to fill them with photons. As a result, images in 16 wavelength channels can be recorded at a resolution of 512x512 pixels and 256 time channels. An example is shown in Fig. 15.

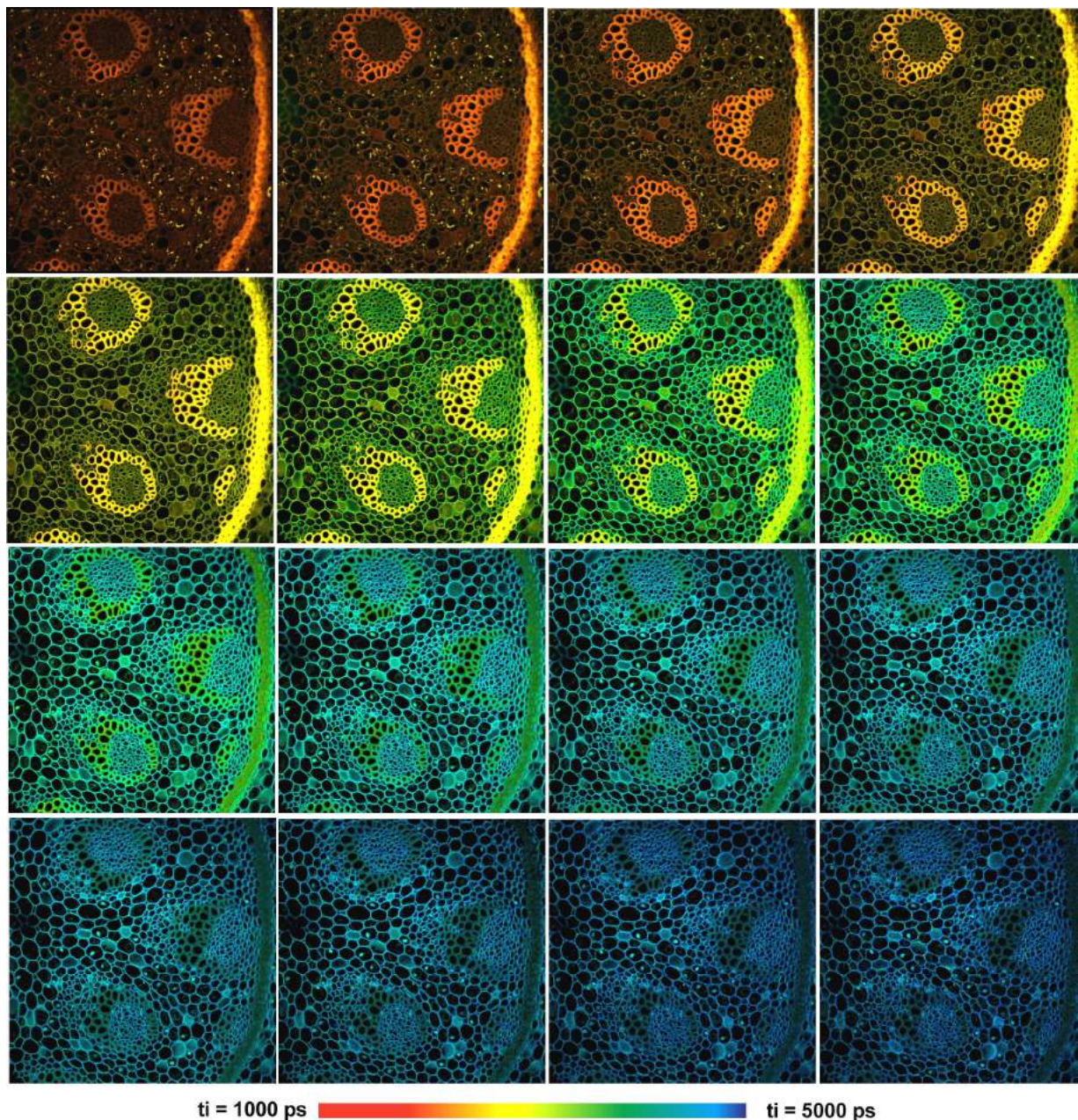


Fig. 15: Multi-wavelength FLIM with the bh MW-FLIM GaAsP 16-channel detector. 16 images with 512 x 512 pixels and 256 time channels were recorded simultaneously. Wavelength from upper left to lower right, 490 nm to 690 nm, 12.5 nm per image. DCS-120 confocal scanner, Zeiss Axio Observer microscope, x20 NA=0.5 air lens.

Fig. 16 demonstrates the true spatial resolution of the data. Images from two wavelength channels, 502 nm and 565 nm, were selected from the data shown Fig. 15, and displayed at larger scale and with individually adjusted lifetime ranges. With 512x512 pixels and 256 time channels, the spatial and temporal resolution of the individual images is comparable with what previously could be reached for FLIM at a single wavelength. Decay curves for selected pixels of the images are shown in Fig. 17.



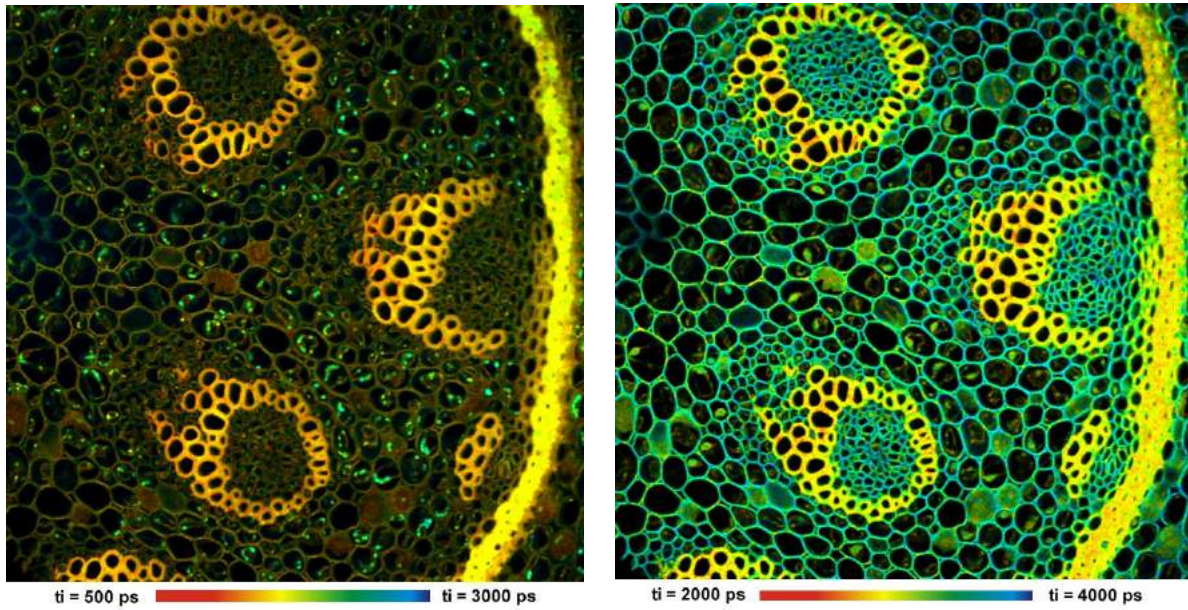


Fig. 16: Two images from the array shown in Fig. 15, displayed in larger scale and with individually adjusted lifetime range. Wavelength channels 502 nm (left) and 565 nm (right). The images have 512 x 512 pixels and 256 time channels.

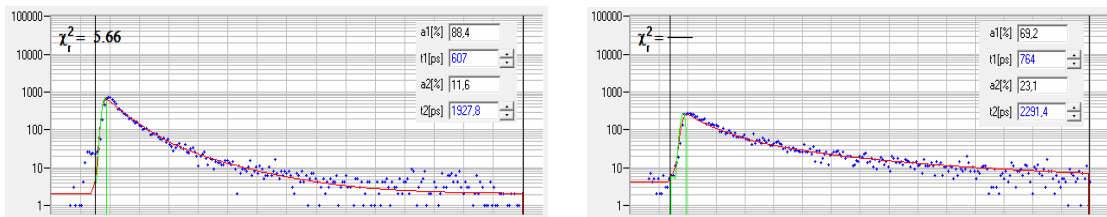


Fig. 17: Decay curves at selected pixel position in the images shown above. Blue dots: Photon numbers in the time channels. Red curve: Fit with a double-exponential model.

### Z Stack Recording by Record-and-Save Procedure

In combination with the Zeiss Axio Observer Z1 microscope the DCS-120 system is able to record z-stacks of FLIM images. The sample is continuously scanned. For each plane, a FLIM image is acquired for a specified 'collection time'. Then the data are saved in a file, the microscope is commanded to step to the next plane, and the next image is acquired. The procedure continues for a specified number of Z planes. A Z stack of autofluorescence images taken at a water flea is shown in Fig. 18.

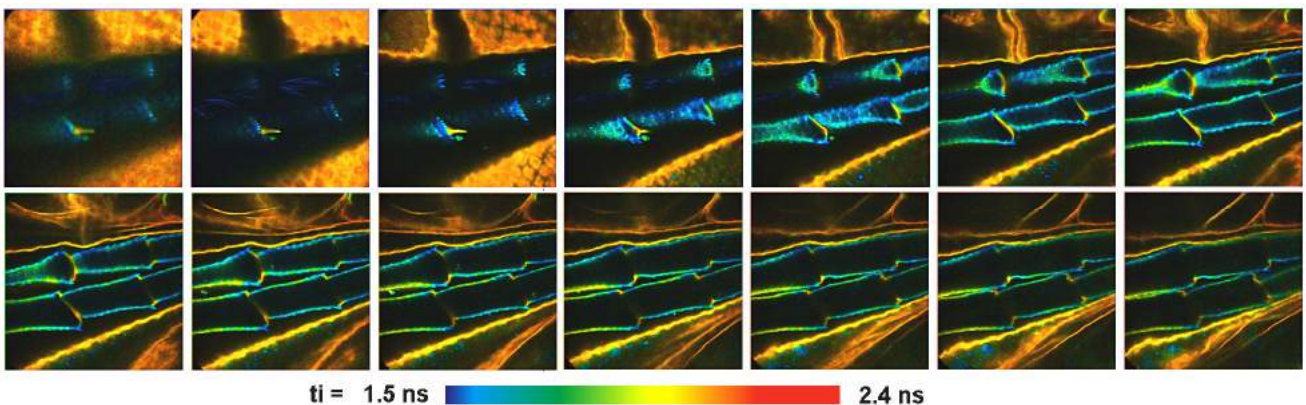


Fig. 18: Z stack recording, part of a water flea, autofluorescence. 15 steps in Z, step width 4  $\mu$ m.



### Z-Stack recording by Mosaic FLIM

Z Stacks of FLIM images can be recorded by the Mosaic FLIM function of the 64 bit SPCM software. As the microscope scans consecutive images planes in the sample the FLIM system records the data into consecutive elements of a FLIM mosaic. Two such mosaic data sets are obtained simultaneously through the two channels of the DCS system. The advantage over the traditional record-and-save procedure is that no time has to be reserved for save operations, and that the entire array can be analysed in a single data analysis run.

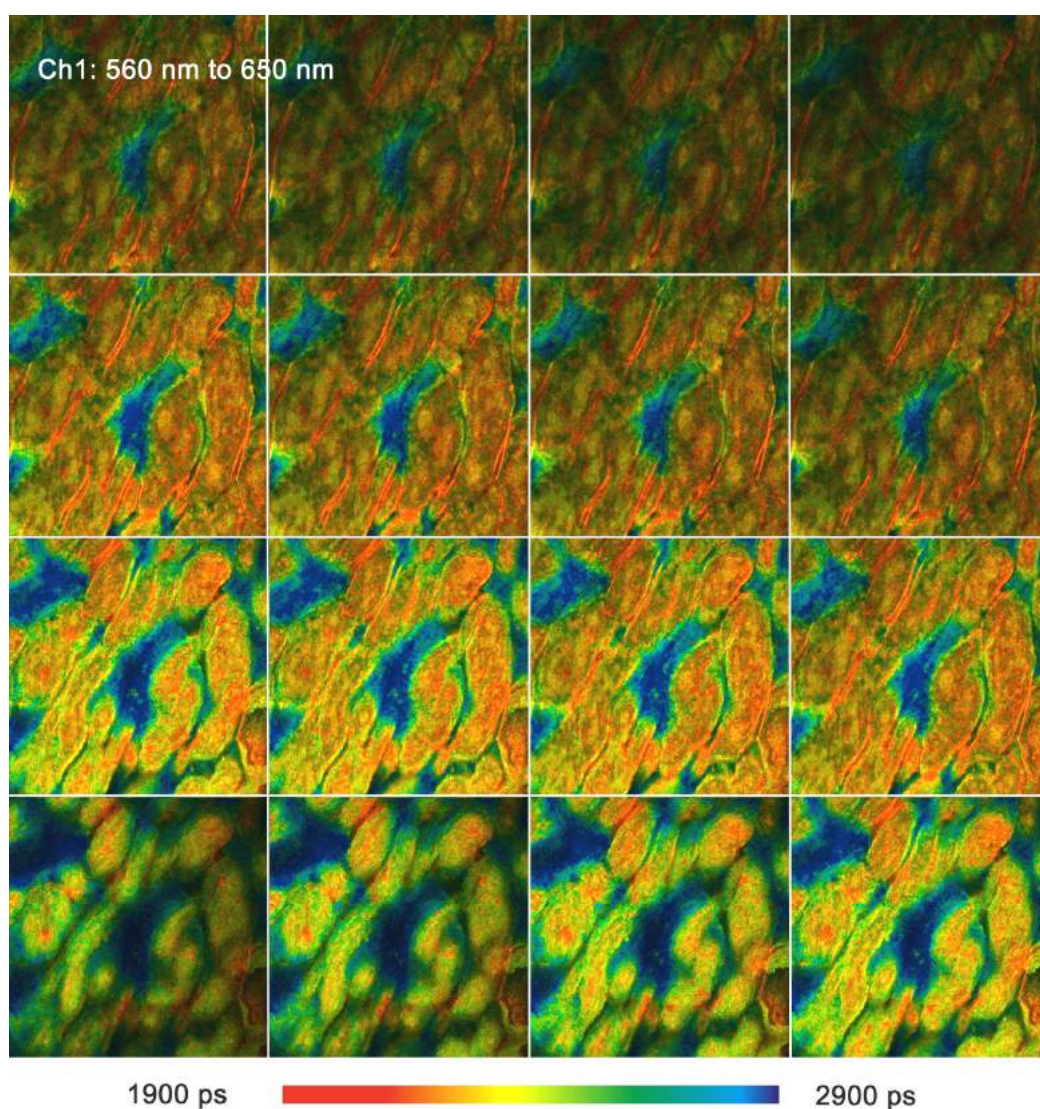


Fig. 19: FLIM Z-stack, recorded by Mosaic FLIM. Pig skin, autofluorescence. 16 planes, 0 to 30  $\mu\text{m}$  from top of the tissue. Each element of the FLIM mosaic has  $512 \times 512$  pixels and 256 time channels per pixel.

### Time-Series FLIM by Record-and-Save Procedure

Time-series FLIM by the traditional record-and-save procedure is available for all DCS-120 system versions. With the SPC-152 dual-channel systems time series as fast as 2 images per second can be obtained [34]. A time series taken at a moss leaf is shown in Fig. 20. The fluorescence lifetime of the chloroplasts changes due to the Kautski effect induced by the illumination.

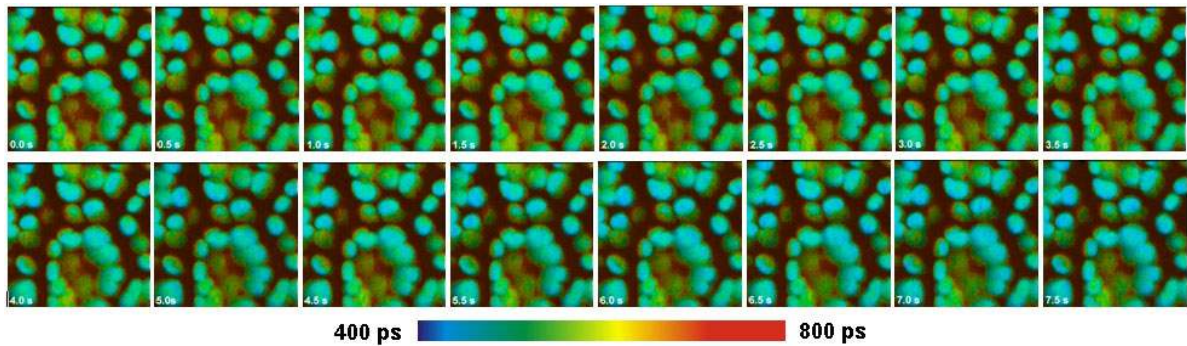


Fig. 20: Time-series FLIM, 2 images per second. Chloroplasts in a leaf, the fluorescence lifetime of the chlorophyll decreases with the time of exposure.

### Time-Series Recording by Mosaic FLIM

SPCM 64-bit software versions later than 2014 have a ‘Mosaic Imaging’ function implemented. For time-series recording, subsequent frames of the scan are recorded into subsequent elements of the mosaic. The sequence can be repeated and accumulated [21, 24]. The time per mosaic element can be as short as a single frame, which can be less than 100 ms. Another advantage is that the entire array can be analysed in a single SPCImage data analysis run. Fig. 21 shows the change of the lifetime of chlorophyll in plant tissue with the illumination.

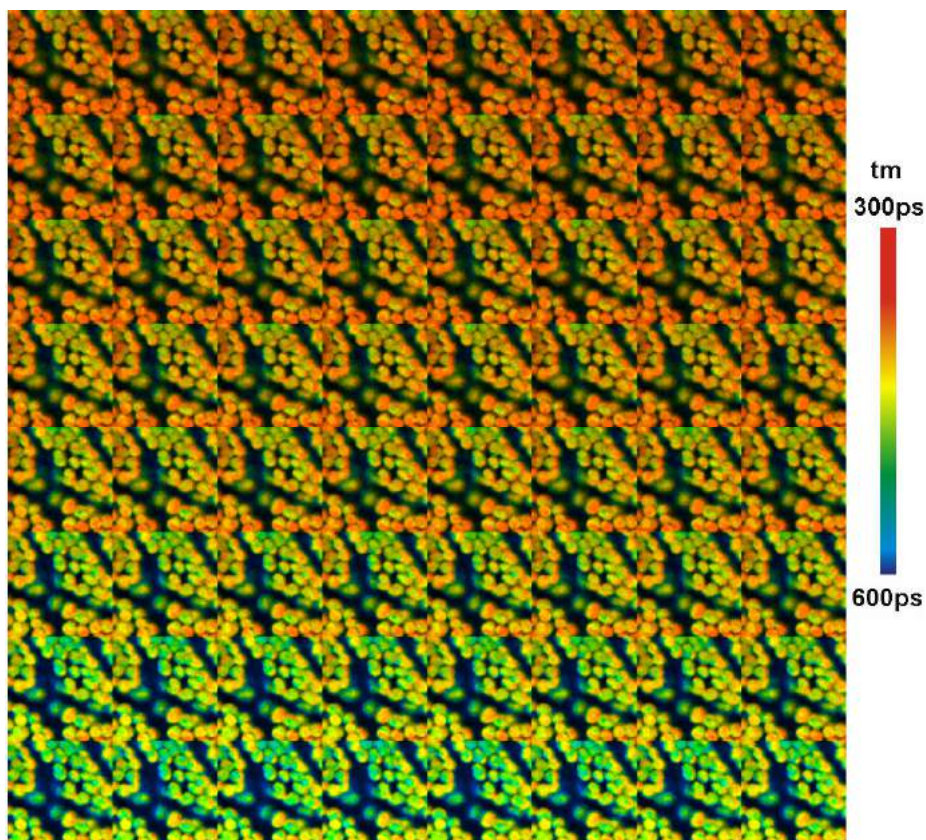


Fig. 21: Time series of chloroplasts in a leaf recorded by Mosaic Imaging. 64 mosaic elements, each 128x128 pixels, 256 time channels. Scan time per element 1s. Experiment time from lower left to upper right. Amplitude-weighted lifetime of double-exponential decay.



### Laser Wavelength Multiplexing

The two ps-diode lasers of the DCS-120 system can be multiplexed on a pixel-by-pixel, line-by-line, or frame-by-frame basis. With the two detection channels of the DCS system, images for three or four combinations of excitation and emission wavelength are obtained. An example is shown in Fig. 22.

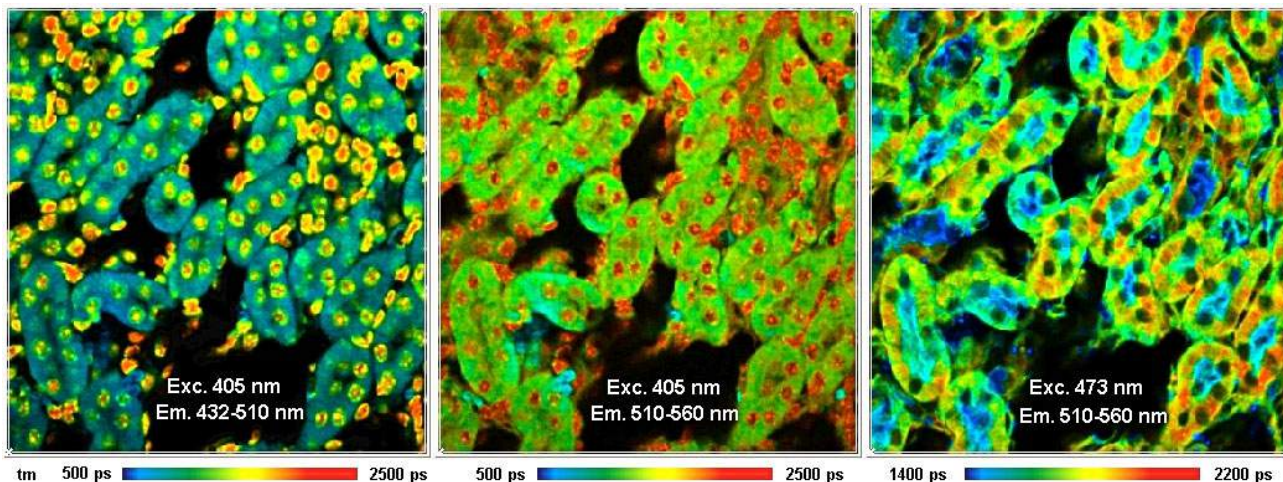


Fig. 22: Excitation wavelength multiplexing, 405 nm and 473 nm. Detection wavelength 432 nm to 510 nm and 510 nm to 550 nm. Mouse kidney section, stained with Alexa 488 WGA, Alexa 568 phalloidin, and DAPI.

### Tunable Excitation

The DCS-120 WB wideband version can be used with tuneable excitation. Images obtained with a Toptica Ichrome laser are shown in Fig. 23.

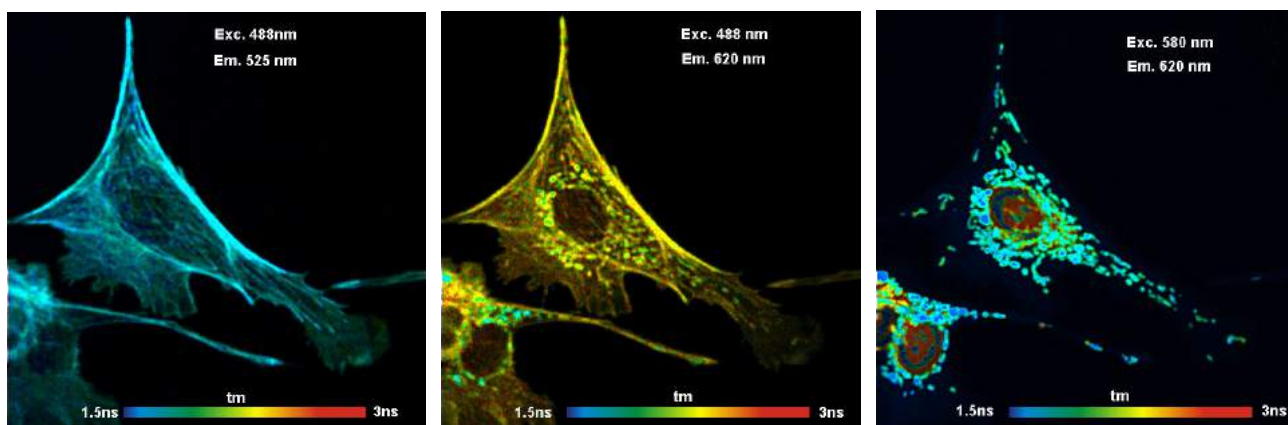


Fig. 23: Tuneable excitation with DCS-120 WB and Toptica Ichrome laser. Left to right: Excitation 488 nm emission 525±15 nm, excitation 488 nm emission 620±30 nm, and excitation 580 nm emission 620±30 nm.

### Multiphoton FLIM

With a femtosecond titanium-sapphire laser the DCS-120 system converts into a multiphoton microscope. Multiphoton excitation penetrates deep into biological tissue. Moreover, excitation occurs only in the focus of the laser. The fluorescence can therefore be detected by a non-descanned detector [8]. Fluorescence photons scattered on the way out of the sample are thus detected more efficiently than in a confocal system. The result is that clear images are obtained from deep tissue layers.



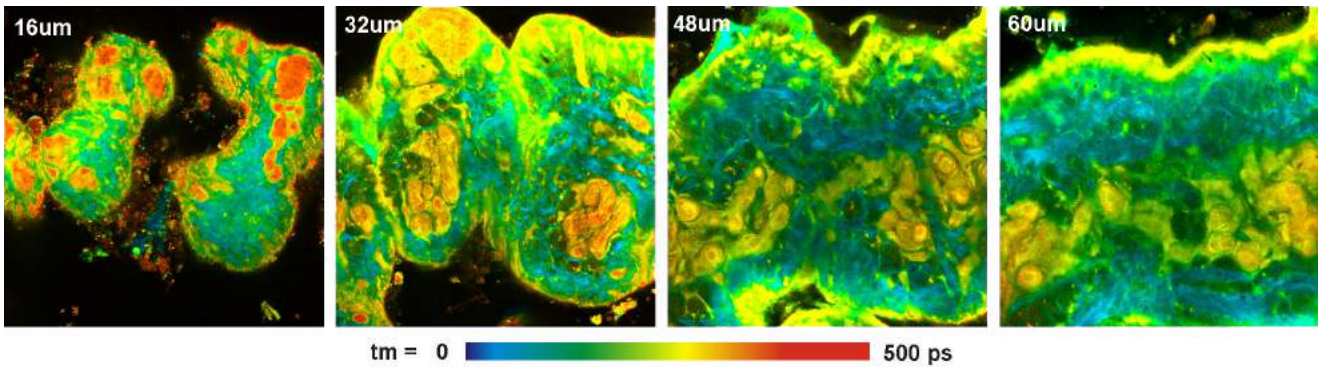


Fig. 24: Pig skin, autofluorescence, image in different depth in the sample. Amplitude-weighted lifetime of triple-exponential decay model. Excitation 805 nm, 512x512 pixels, 256 time channels. Zeiss Axio Observer Z1, Water C apochromate NA=1.2, non-descanned detection, HPM-100-40 hybrid detector.

### *Near-Infrared FLIM*

The DCS-120 WB version is able to record lifetime images with near-infrared fluorophores. An image of a pig skin sample incubated with 3,3'-diethylthiatricarbocyanine is shown in Fig. 25.

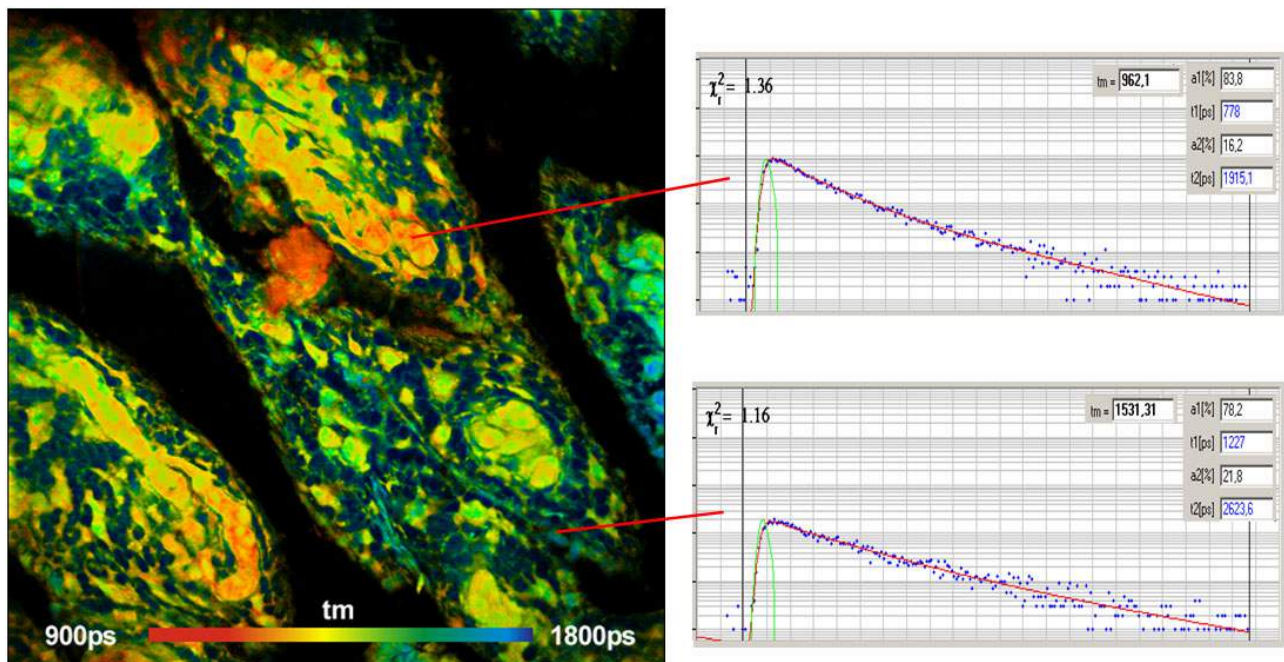


Fig. 25: Near-Infrared FLIM. Pig skin sample stained with 3,3'-diethylthiatricarbocyanine, detection wavelength from 780 nm to 900 nm.

### *FLIM / PLIM: Simultaneous Fluorescence and Phosphorescence Lifetime Imaging*

Phosphorescence and fluorescence lifetime images are recorded simultaneously by bh's proprietary FLIM/PLIM technique. The technique is based on modulating a ps diode laser synchronously with the pixel clock of the scanner [18, 21]. FLIM is recorded during the 'On' time, PLIM during the 'Off' time of the laser. The SPCM software delivers separate images for the fluorescence and the phosphorescence which are then analysed with SPCImage FLIM/PLIM analysis software.

Currently, there is increasing interest in PLIM for background-free recording and for oxygen sensing [1, 2, 29, 30, 35, 37, 41]. In these applications, the bh technique delivers a far better sensitivity than PLIM techniques based on single-pulse excitation. The real advantage of the FLIM/PLIM technique

used in the DCS-120 is, however, that FLIM and PLIM are obtained *simultaneously*. It is thus possible to record metabolic information via FLIM of the NADH and FAD fluorescence, and simultaneously map the oxygen concentration via PLIM. An example is shown in Fig. 26.

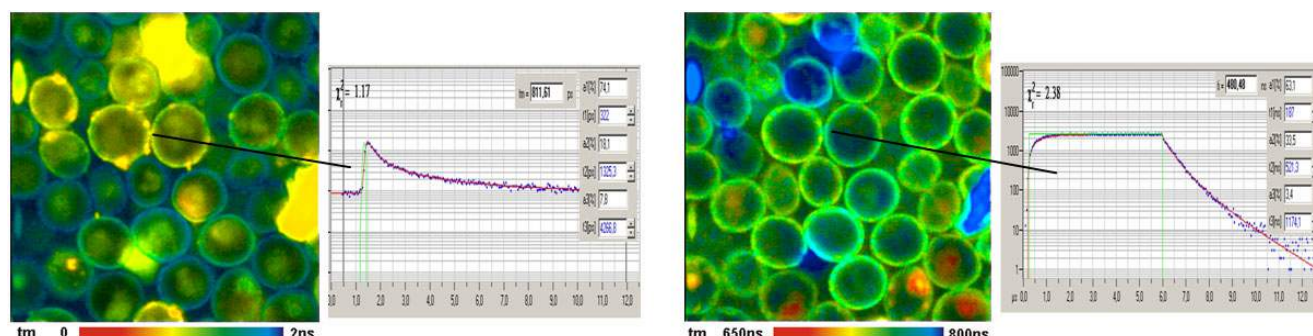


Fig. 26: Yeast cells stained with (2,2'-bipyridyl) dichlororuthenium (II) hexahydrate. FLIM and PLIM image, decay curves in selected spots.

PLIM can also be interesting for the investigation the luminescence properties of inorganic compounds. The emission can come almost entirely from energy levels of extremely long lifetime. An example is shown in Fig. 27.

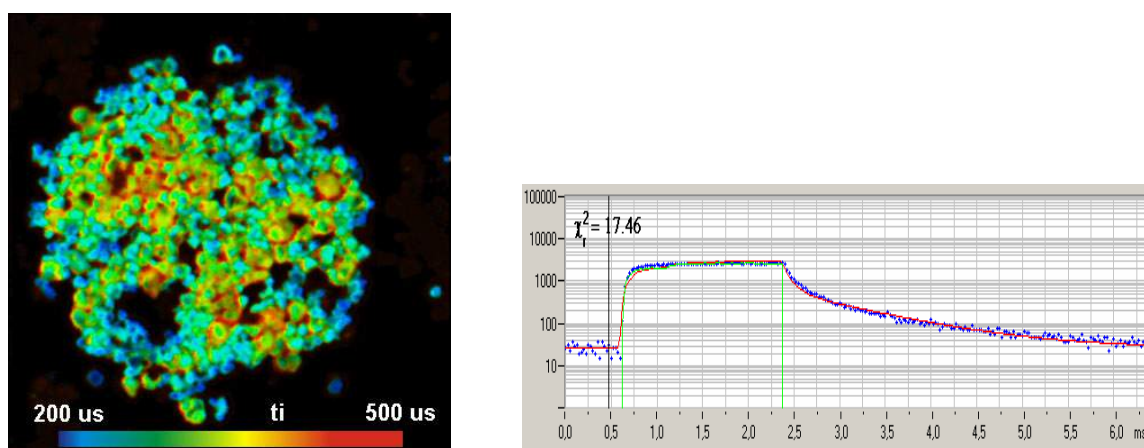


Fig. 27: Phosphorescence lifetime imaging of a luminophor for a cathode-ray tube. Left: Lifetime image. Right: Phosphorescence decay curve at selected position within the image

### FLITS: Fluorescence Lifetime-Transient Scanning

FLITS records transient effects in the fluorescence lifetime of a sample along a one-dimensional scan. The technique is based on building up a photon distribution over the distance along the scan, the arrival times of the photons after the excitation pulses, and the experiment time after a stimulation of the sample. The maximum resolution at which lifetime changes can be recorded is given by the line scan time. With repetitive stimulation and triggered accumulation transient lifetime effects can be resolved at a resolution of about one millisecond [21, 22, 33]. This is enough to record transient changes in the concentration of free  $\text{Ca}^{2+}$  in live neurons, as has been demonstrated in [22, 33].



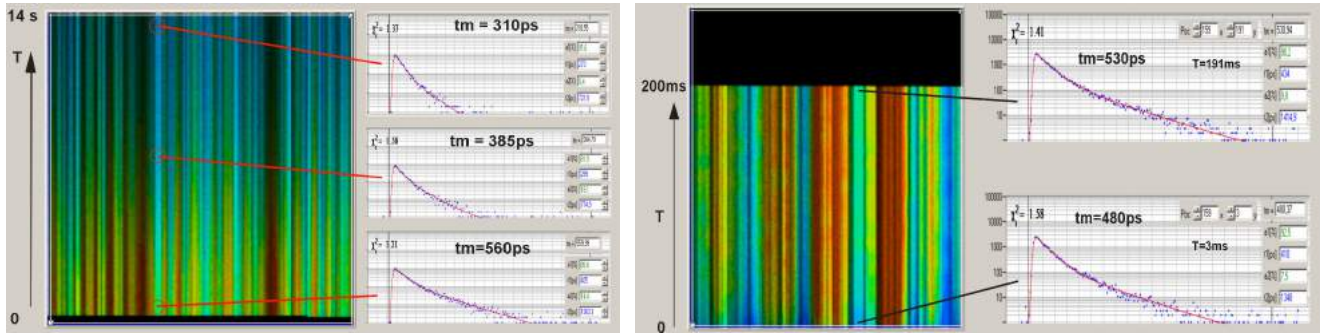


Fig. 28: FLITS of chloroplasts in a grass blade, change of fluorescence lifetime after start of illumination. Left: Non-photochemical transient, transient resolution 60 ms. Right: Photochemical transient. Triggered accumulation, transient resolution 1 ms.

### Imaging of Macroscopic Objects

The DCS MACRO version of the DCS system scans objects directly in the focal plane of the scanner. Objects up to a size of 12 mm can be imaged at high resolution. Fig. 29 shows a leaf with a fungus infections.

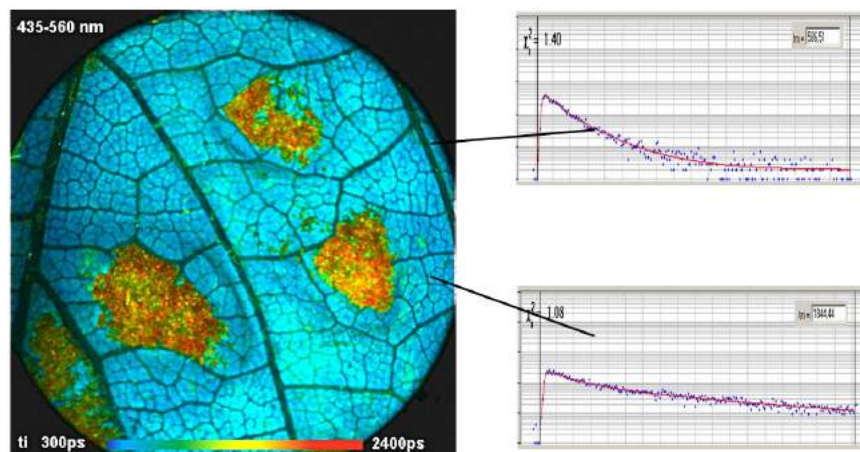


Fig. 29: Leaf with a fungus infection. ps diode laser excitation, 405nm, scan format 512 x 512 pixels. Right: Decay functions of healthy and infected areas.

### FLIM through Endoscopes

The DCS-120 Macro can be combined with endoscopes. Optical details are described in [3]. Images of (benign) human skin lesions are shown in ???

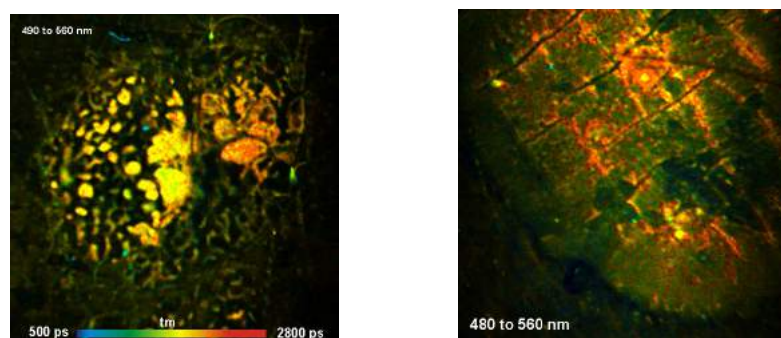


Fig. 30: Basal cell papilloma (left) and a keratotic lesion (right), scanned in vivo through a rigid endoscope. Excitation wavelength 405 nm, detection wavelength 480 to 560 nm. Excitation power 50  $\mu$ W, acquisition time 10 seconds.

### FCS

Due to the superior performance of the HPM-100-40 hybrid detectors the DCS-120 system delivers highly efficient FCS. There is no afterpulsing peak in autocorrelation data [4]. Thus, accurate diffusion times and molecular-brightness parameters are obtained from a single detector. Compared to cross-correlation of split signals, correlation of single-detector signals yields a four-fold increase in correlation efficiency. The result is a substantial improvement in the SNR of FCS recordings [21]. Gated FCS is possible by hardware gating via the TAC limits of the TCSPC modules, FCCS by cross-correlating the signals of the two DCS channels [3, 21].

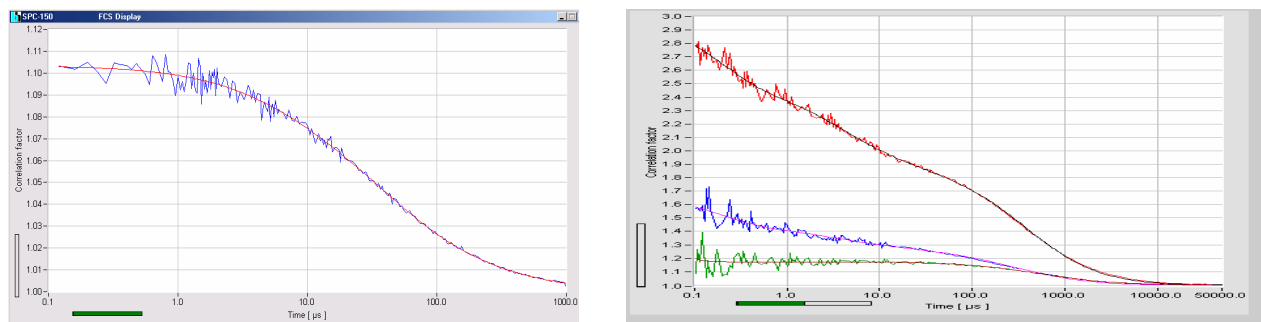


Fig. 31: Left: FCS curve recorded by a single HPM-100 detector. The data are free of an afterpulsing peak. Right: Dual-colour FCS, autocorrelation blue and red, cross-correlation green. Online fit with FCS procedures of SPCM software.



## SPCImage FLIM and PLIM Data Analysis

Data analysis is performed by the bh SPCImage data analysis package, see Fig. 32. Data analysis can be run over a single FLIM or PLIM image, over several images obtained in parallel TCSPC channels, or over the images recorded in the 16 channels of a multi-wavelength system. SPCImage runs an iterative de-convolution and fit procedure on the decay data in the pixels of the images. Single-double, and triple-exponential decay exponential models are available. Residual fluorescence from previous laser pulses can be accounted for by incomplete decay models. Multi-exponential decay analysis can be performed with free or fixed lifetimes of the decay components. SPCImage is able to calculate the instrument-response function (IRF) automatically from the decay data. It can, however, also use a recorded IRF, extract an IRF from SHG signals present in the data, or use a manually defined IRF.

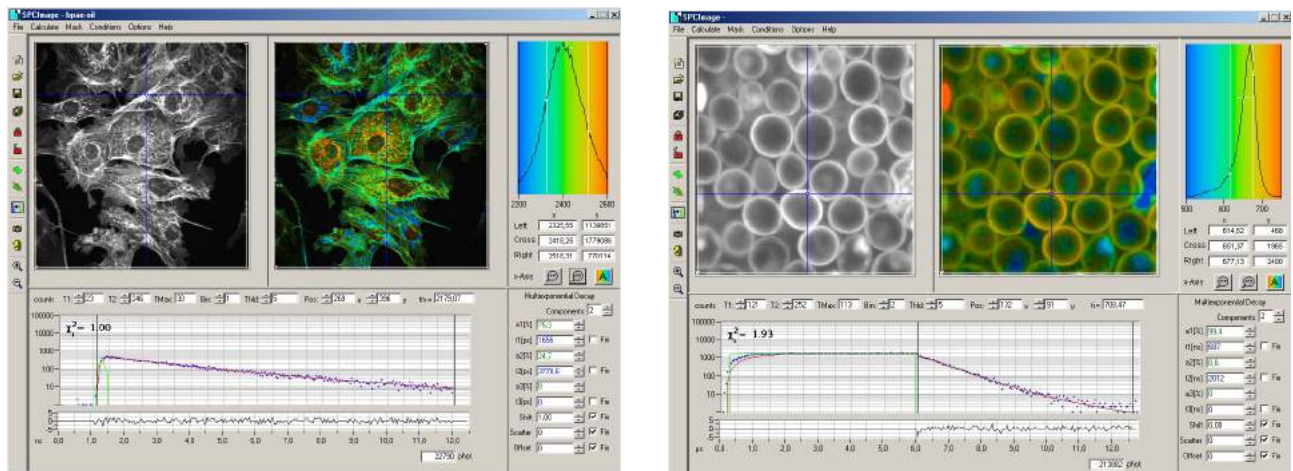


Fig. 32: SPCImage data analysis. Left: FLIM. Right: PLIM

Lifetime data are displayed as false-colour images of the lifetimes or amplitudes of the decay components, or ratios of lifetimes or amplitudes. Moreover, SPCImage is able to calculate and display FRET efficiencies from double-exponential decay data obtained in FRET experiments [3, 11, 21]. The data can be exported into ASCII, BMP, and TIF files.

Batch processing of FLIM file series has been introduced in 2012 [3, 21]. A large number of data files can be specified, analysed with identical model and fit control parameters, and displayed with identical colour and display range parameters. For the results of batch processing a batch export routine is implemented.

Histograms of decay parameters can be displayed in selected regions of interest, see Fig. 33. Since 2013, a two-dimensional histogram function and a phasor plot are implemented. In these histograms, regions of lifetimes, amplitudes or phasor values can be selected, and the corresponding pixels be highlighted in the images. For further details of SPCImage data analysis please see [3, 11, 21].

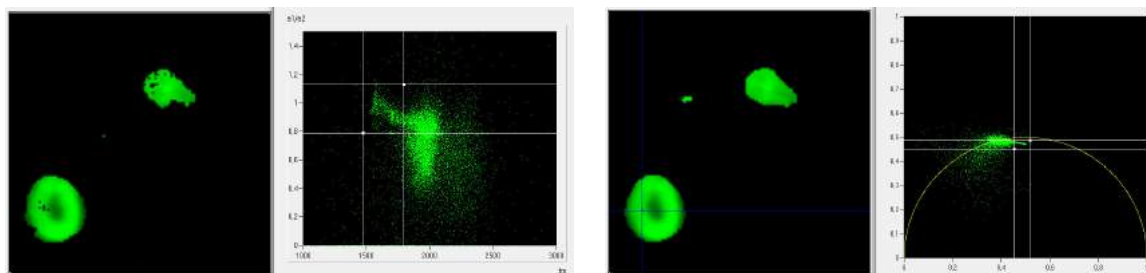


Fig. 33: Images and 2D histograms. Left: amplitude ratio versus amplitude-weighted lifetime. Right: Phasor plot.

## ‘Burst Analyzer’ Single-Molecule Data Analysis

The bh ‘Burst Analyser’ software is used for data analysis of single-molecule fluorescence. It uses parameter-tag data files recorded in the FIFO mode of the SPC-630, SPC-830, SPC-130EM, SPC-150, SPC-150N, or SPC-160 TCSPC modules. Photon bursts from single molecules travelling through a femtoliter detection volume are identified in the parameter-tag data. Within the bursts, intensities, intensity variations, fluorescence lifetimes, and ratios of these parameters between several detection channels of a routing system, different channels of a multi-module TCSPC system, or different time windows of a PIE recording are determined, and histograms of the parameters are calculated. The results are used to obtain histograms and time traces of FRET efficiencies, and to calculate FCS and FCCS data. The Burst Analyser is described in a separate handbook, see [12].

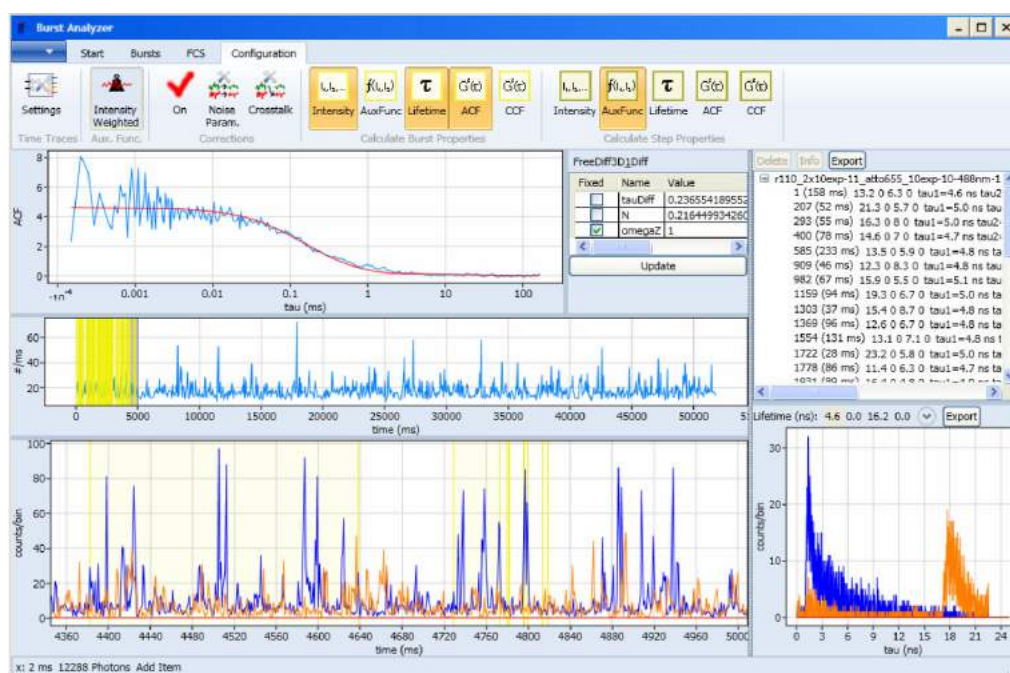


Fig. 34: bh Burst Analyzer software for single-molecule data analysis

## Other Data Analysis Software

DCS-120 data are compatible with other analysis packages. They can be imported into multi-parameter FLIM analysis [28, 31, 42] and phasor analysis [28] in the frequency domain. Single-photon parameter-tag data can be analysed by the bh ‘Burst Analyser’ software. This software is able to identify single-molecule photon bursts in the parameter-tag data, analyse fluorescence lifetimes and intensities within the burst, and build up one- and two-dimensional histograms of the parameters. The results can be used to identify different fluorescent species or different FRET states of single molecules. Moreover, the burst data can be used to calculate FCS and cross-FCS, and fit the curves with standard or user-defined model functions.



## Typical Applications

The advantage of FLIM over other fluorescence imaging techniques is that the fluorescence lifetime of a fluorophore depends on its molecular environment but not on the concentration [17], see Fig. 35. If fluorescence in a sample is excited (Fig. 35, left) the emission intensity depends both on the concentration of the fluorophore and on possible interaction of the fluorophore with its molecular environment. Changes in the concentration, cannot be distinguished from changes in the molecular environment. Spectral measurements (second right) are able to distinguish between different fluorophores. However, changes in the local environment usually do not cause changes in the shape of the spectrum. The fluorescence lifetime of a fluorophore (Fig. 35, right), within reasonable limits, does not depend on the concentration but systematically changes on interaction with the molecular environment.

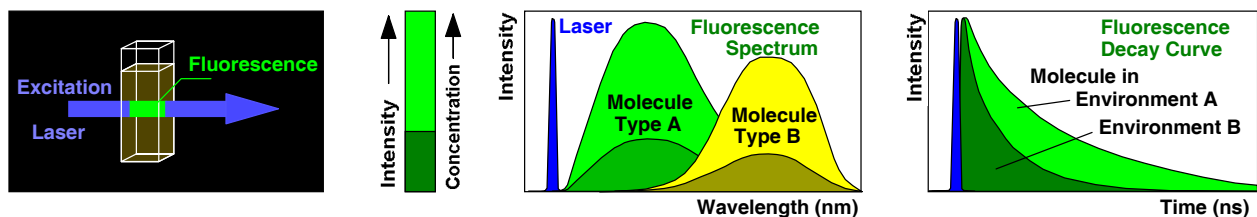


Fig. 35: Fluorescence. Left to right: Excitation light is absorbed by a fluorophore, and fluorescence is emitted at a longer wavelength. The fluorescence intensity varies with concentration. The fluorescence spectrum is characteristic of the type of the fluorophore. The fluorescence decay function is an indicator of interaction of the fluorophore with its molecular environment.

By using the fluorescence lifetime, or, more precisely, the shape of the fluorescence decay function, molecular effects can therefore be investigated independently of the unknown and usually variable fluorophore concentration [21, 25, 36]. Common FLIM applications are ion concentration measurements, probing of protein interaction via FRET, and the probing of metabolic activity and cell viability via the fluorescence lifetimes of NADH and FAD. FLIM may also find application in plant physiology because the fluorescence lifetime of chlorophyll changes with the photosynthesis activity.

### *Förster Resonance Energy Transfer: FRET*

A particularly efficient energy transfer process is Förster resonance energy transfer, or FRET. The effect was found by Theodor Förster in 1946 [32]. FRET is a dipole-dipole interaction of two molecules in which the emission band of one molecule overlaps the absorption band of the other. In this case the energy from the first molecule, the donor, transfers into the second one, the acceptor, see Fig. 36, left. FRET results in an extremely efficient quenching of the donor fluorescence and, consequently, in a considerable decrease of the donor lifetime, see Fig. 36, right.

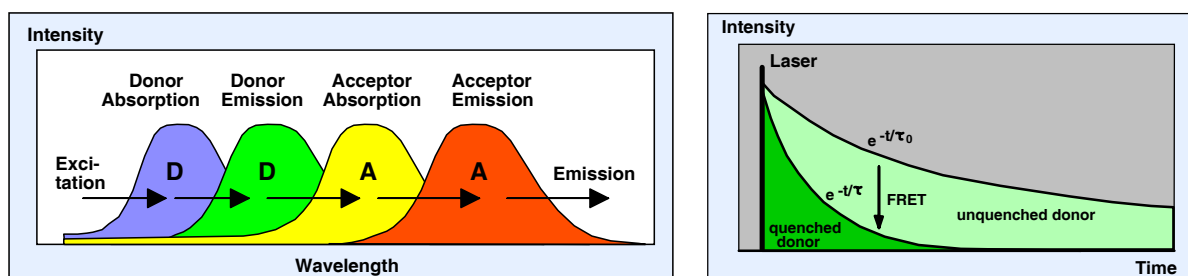


Fig. 36: Fluorescence Resonance Energy Transfer (FRET)

The energy transfer rate from the donor to the acceptor increases with the sixth power of the reciprocal distance. Therefore it is noticeable only at distances shorter than 10 nm [36]. FRET is used as a tool to

investigate protein-protein interaction. Different proteins are labelled with the donor and the acceptor, and FRET is used as an indicator of the binding between these proteins. Steady-state FRET measurements have the problem that the relative concentration of donor and acceptor varies, that the donor emission spectrally extends into the acceptor emission, and that a fraction of the acceptor is excited directly. FLIM does not have these problems because all it needs is to record a lifetime image at the donor emission wavelength. FRET is the most frequent FLIM application, please see [21] for references.

Fig. 37 shows FRET in a cultured live HEK cell. The cell is expressing two proteins, one labelled with CFP, the other with YFP. FRET occurs in the places where the proteins interact. The associated changes in the donor lifetime are clearly visible in the lifetime image shown in Fig. 37, left.

FLIM is not only able to detect FRET without interference by donor and acceptor bleedthrough, it even delivers independent images of the donor-acceptor distance and the fraction of interacting donor. Such images can be obtained by double-exponential analysis of the FLIM data: The interacting donor fraction delivers a fast, the non-interacting fraction a slow decay component. The ratio of the two lifetimes is directly related to the donor-acceptor distance, the ratio of the amplitudes of the components is the ratio of interacting and non-interacting donor. Images which resolve these two parameters of the FRET system are shown in Fig. 37, middle and right.

Remarkably, double exponential FRET does not need an external lifetime reference: The reference lifetime is the slow decay component, originating from the non-interaction donor. Please see [3, 15, 21] for details and for further references.

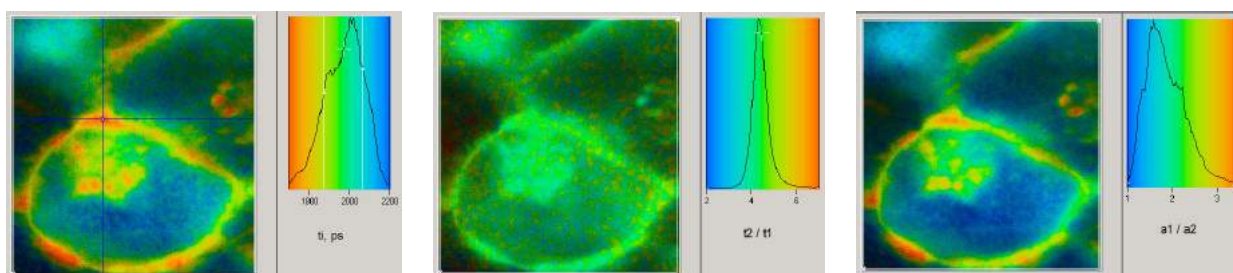


Fig. 37: FRET in HEK cell expressing proteins labelled with CFP and YFP. Left: Lifetime image at donor wavelength, showing lifetime changes by FRET. Middle and right: FRET results obtained by double-exponential lifetime analysis. Ratio of the lifetimes of the decay components,  $t_2/t_1 = \tau_0/\tau_{\text{fret}}$ , and ratio of the interacting and non-interacting donor fractions,  $a_1/a_2 = N_{\text{fret}}/N_0$ .

## Autofluorescence

Biological tissue contains a wide variety of endogenous fluorophores [38]. However, the fluorescence spectra of endogenous fluorophores are broad, variable, and poorly defined. Moreover, absorbers present in the tissue may change the apparent fluorescence spectra. It is therefore difficult to disentangle the fluorescence components by their emission spectra alone. Autofluorescence lifetime detection is expected to add an additional separation parameter to the analysis of the data.

More important, the autofluorescence intensities and lifetimes contain information about the binding, the metabolic state and the microenvironment of the fluorophores. Especially interesting are the fluorescence signals from coenzymes, such as flavin adenine nucleotide (FAD) and nicotinamide adenine dinucleotide (NADH). It is known that the fluorescence lifetimes of NADH and FAD depend on the binding [36]. The lifetimes, the ratio of bound and unbound NADH, and the NADH / FAD intensity ratio also depend on the metabolic state [27], and on the redox state [26]. The NADH and FAD fluorescence intensities and lifetimes are therefore used to detect precancerous and cancerous alterations [39]. For an overview about the literature please see [21].



Fig. 38 shows an example of how autofluorescence signals change with the oxygen concentration. Yeast cells were kept in a sugar solution. They produce  $\text{CO}_2$  which washes out the oxygen from the solution. The left image was recorded under such conditions. Only a few cells are visible Fig. 38, left and middle, the other ones are extremely dim. The image in Fig. 38, right, was recorded after the solution had been saturated with oxygen. The difference in the fluorescence behaviour is striking.

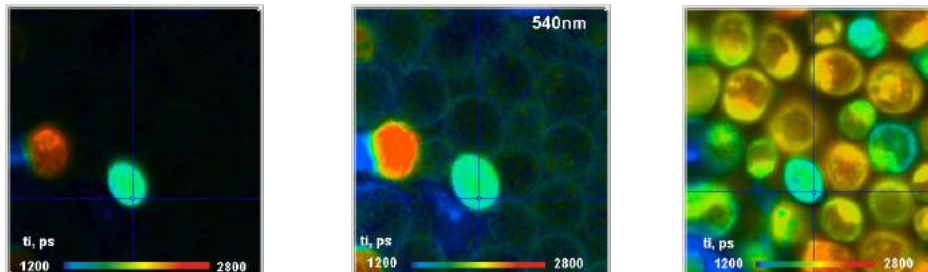


Fig. 38: Autofluorescence of yeast cells. Left and middle: Saturated with  $\text{CO}_2$ , different intensity scale of the same data set. Right: Saturated with  $\text{O}_2$ . Excitation 405 nm, detection at 540 nm.

Fig. 39 shows a pig skin autofluorescence image obtained at 405 nm excitation wavelength. Due to the absence of exogenous fluorophores the fluorescence intensity is low. Nevertheless, the FLIM data contain enough photons for double-exponential decay analysis. The image on the left shows the amplitude-weighted mean lifetime,  $t_m$ . The image in the middle shows the ratio of the intensities,  $q_1/q_2$ , contained in the fast and the slow decay component. Two typical decay curves are shown on the right.

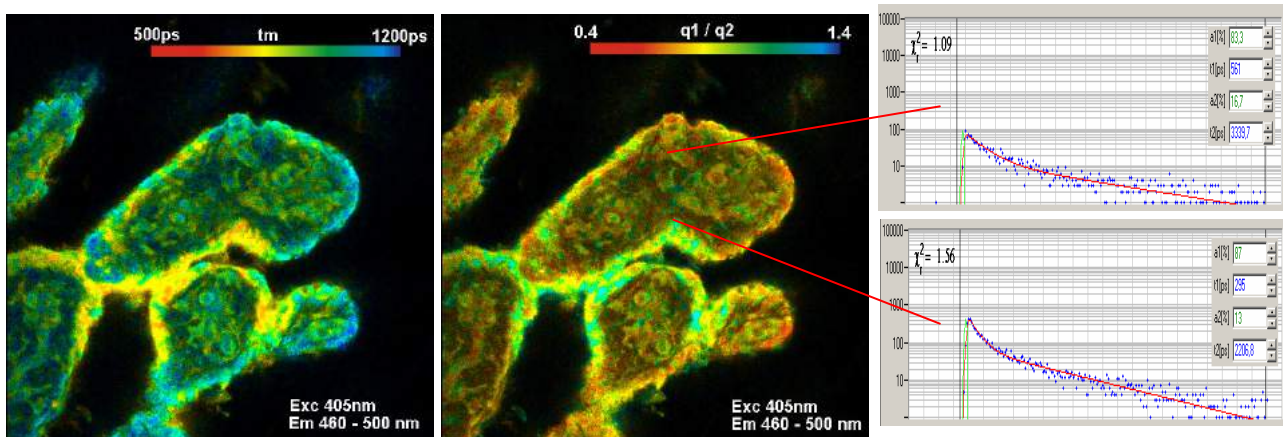


Fig. 39: Pig skin sample excited at 405 nm, detection from 460 to 500 nm. Double-exponential fit. Left: Amplitude-weighted lifetime. Middle: Intensity ratio of fast and slow decay component. Right: Decay curves in two spots of the image.

In the wavelength interval recorded the emission can be expected to be dominated by NADH fluorescence. The lifetimes of bound and unbound NADH are different. The  $q_1/q_2$  ratio can therefore be expected to represent the intensity ratio of bound and unbound NADH. It should be noted that accurate NADH analysis, of course, requires spectral unmixing of the NADH signal from contributions of other fluorophores [27]. Due to the variability of the autofluorescence spectra and lifetimes, fluorescence contribution from other fluorophores, and the presence of unknown absorbers the task is extremely complicated. The prospects of unmixing the signals improve considerably with the availability of excitation wavelength multiplexing (Fig. 22, page 16) or tuneable excitation Fig. 23, page 16.

### Plant Physiology

Two examples of FLIM of plant tissue are shown in Fig. 40 and Fig. 41. The fluorescence is dominated by the fluorescence of chlorophyll and the fluorescence of flavines. Multi-wavelength FLIM images of a moss leaf recorded with the bh multi-spectral FLIM detector are shown in Fig. 40.

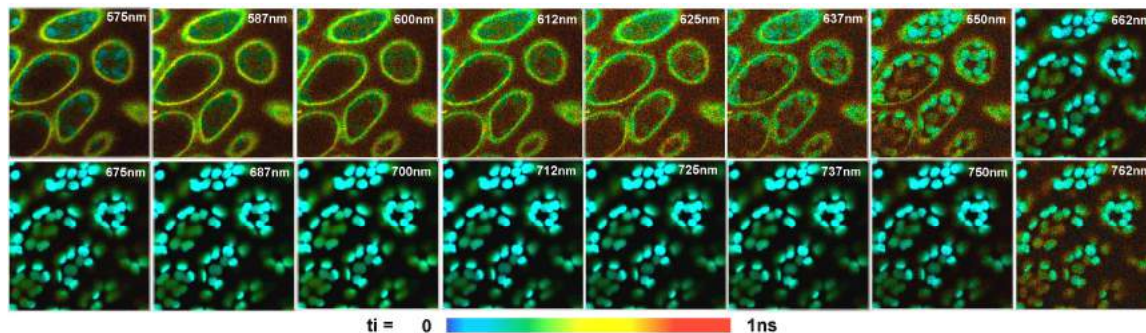


Fig. 40: Multi-spectral FLIM of plant tissue. Moss leaf, excitation at 405 nm, wavelength from 575 nm to 762 nm. DCS-120, MW FLIM detector. Image size 256x256 pixels, 64 time channels, 16 wavelength channels.

The fluorescence of chlorophyll competes with the energy transfer into the photosynthesis channels. Thus, the fluorescence lifetime and its change on illumination is a sensitive indicator of the photosynthesis efficiency. The change in the fluorescence lifetime of the chloroplasts in a moss leaf on exposure to light can be recorded by time-series FLIM, see Fig. 41.

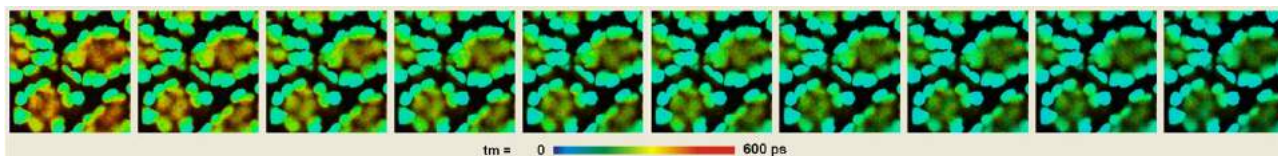


Fig. 41: Change of the fluorescence lifetime of chlorophyll with time of exposure. Moss leaf, excitation at 445 nm, 256x256 pixels, 1 image per second.

Faster effects down to the millisecond time scale can be recorded by temporal mosaic FLIM or FLITS.

### Summary

The DCS-120 system records lifetime images at high spatial and temporal resolution, extremely high sensitivity, and short acquisition time. Recently introduced 64-bit SPCM operating software has increased the image format of FLIM into the megapixel region. Single-, dual-, multi-wavelength FLIM is now recorded at unprecedented image quality. Moreover, the large memory space available in the 64 bit environment made it possible to implement advanced FLIM techniques, like time series recording and Z stack recording by Mosaic recording. Physiological effects down to the millisecond range can be resolved by triggered mosaic FLIM and by FLITS. Metabolic effects can be recorded by FLIM and correlated with changes in the oxygen concentration simultaneously measured by PLIM. No other FLIM technique and no other FLIM system offers a similar range of advanced capabilities.



## Specifications

### Scan head

Optical principle	confocal, beam scanning by fast galvanometer mirrors
Laser inputs	two independent inputs, fibre coupled or free beam
Laser power regulation, optical	continuously variable via neutral-density filter wheels
Outputs to detectors	two outputs, detectors are directly attached
Main beamsplitter versions	multi-band dichroic, wideband, multiphoton
Secondary beamsplitter wheel	3 dichroic beamsplitters, polarising beamsplitter, 100% to channel1, 100% to channel2
Pinholes	independent pinhole wheel for each channel
Pinhole size	11 pinholes, from about 0.5 to 10 AU
Emission filters	2 filter sliders per channel
Connection to microscope	adapter to left side port or port on top of microscope
Coupling of lasers into scan head (visible)	single-mode fibres, Point-Source type, separate for each laser
Coupling of laser into scan head (Ti:Sa)	free beam, 1 to 2 mm diameter

### Scan Controller

Principle	Digital waveform generation, scan waveforms generated by hardware
Scan waveform	linear ramp with cycloid flyback
Scan format	line, frame, or single point
Frame size, frame scan	16x16 to 4096x4096 pixels
line scan	16 to 4096 pixels
X scan	continuous or pixel-by-pixel
Y scan	line by line
Laser power control, electrical	via electrical signal to lasers
Laser multiplexing	frame by frame, line by line, or within one pixel
Beam blanking	during flyback and when scan is stopped
Scan rate	automatic selection of fastest rate or manual selection
minimum pixel time for frame size	64x64 128x128 256x256 512x512 1024x1024 2048x2048
Zoom=1	25.6µs 12.8µs 6.4µs 3.2µs 1.6µs 1.2µs
Zoom=8	6.4µs 3.2µs 1.6µs 0.8µs 0.6µs 0.5µs
minimum frame time for frame size	64x64 128x128 256x256 512x512 1024x1024 2048x2048
Zoom=1	0.19s 0.37s 0.64s 1.24s 2.6s 6.5s
Zoom=8	0.037s 0.074s 0.173s 0.320s 1.0s 2.7s
Scan area definition	via zoom and offset or interactive via cursors during preview
Fast preview function	1 second per frame, 128 x 128 pixels
Beam park function	via cursor in preview image or cursor in FLIM image
Laser control	2 Lasers, on/off, frame, line, pxl multiplexing

### Diode lasers

Number of lasers simultaneously operated	bh BDL-SMC or BDL-SMN laser
Wavelengths	2
Pulse width, typical	375nm, 405nm, 445nm, 473nm, 510nm, 640nm, 685nm, 785nm
Pulse frequency	40 to 70 ps
Power in picosecond mode	20MHz, 50MHz, 80MHz, or CW
Power in CW mode	0.25mW to 1mW injected into fibre. Depends on wavelength version.
	10 to 40mW injected into fibre. Depends on wavelength version.

### Other lasers

Visible and UV range	any ps pulsed laser of 20 to 80 MHz repetition rate
Coupling requirements	Point-Source Kineflex compatible fibre adapter
Wavelength	any wavelength from 400nm to 800nm
fs NIR Lasers for multiphoton operation	any fs laser
Coupling requirements	free beam, diameter 1 to 2 mm
Wavelength	740 to 1200 nm

### Detectors (standard)

No. of detectors	bh HPM-100-40 hybrid detector
Spectral Range	2
Peak quantum efficiency	300 to 710nm
IRF width with bh diode laser	40 to 50%
Detector area	120 to 130 ps
Background count rate, thermal	3mm
Background from afterpulsing	300 to 2000 counts per second
Power supply and overload shutdown	not detectable
	via DCC-100 controller of TCSPC system



## DCS-120 FLIM System

### Detectors (optional)

Spectral Range  
 Peak quantum efficiency  
 IRF width with bh diode laser  
 Detector area  
 Background count rate, thermal  
 Background from afterpulsing  
 Overload shutdown  
 Power supply and overload shutdown

### bh HPM-100-50 hybrid detector

400 to 900nm  
 12 to 15%  
 120 to 130 ps  
 3mm  
 1000 to 8000 counts per second  
 not detectable  
 via DCC-100 controller of TCSPC system  
 via DCC-100 controller of TCSPC system

### Detectors (optional)

Spectral range  
 Number of wavelength channels  
 Spectral width of wavelength channels  
 IRF width with bh diode laser  
 Power supply and overload shutdown

### bh MW FLIM GaAsP Multi-Wavelength FLIM detector

380 to 700nm  
 16  
 12.5 nm  
 200 to 250 ps  
 via DCC-100 controller of TCSPC system

### TCSPC System

Number of parallel modules (recording channels)  
 Number of detector (routing) channels in each module  
 Principle  
 Electrical time resolution  
 Minimum time channel width  
 Dead time  
 Saturated count rate  
 Dual-time-base operation  
 Source of macro time clock  
 Input from detector  
 Reference (SYNC) input  
 Synchronisation with scanning  
 Scan rate  
 Synchronisation with laser multiplexing  
 Recording of multi-wavelength data  
 Basic acquisition principles

### bh SPC-150 or SPC-150N modules, see [21] for details

2  
 16  
 Advanced TAC/ADC principle [21]  
 2.3 ps rms  
 813 fs  
 100 ns  
 10 MHz per channel  
 via micro times from TAC and via macro time clock  
 internal 40MHz clock or from laser  
 constant-fraction discriminator  
 constant-fraction discriminator  
 via frame clock, line clock and pixel clock pulses  
 any scan rate  
 via routing function  
 simultaneous, via routing function  
 on-board-buildup of photon distributions  
 buildup of photon distributions in computer memory  
 generation of parameter-tagged single-photon data  
 online auto or cross correlation and PCH  
 f(t), oscilloscope, f(txy), f(t,T), f(t) continuous flow  
 FIFO (correlation / FCS / MCS) mode  
 Scan Sync In imaging, Scan Sync In with continuous flow  
 FIFO imaging, with MCS imaging, mosaic imaging, time-series imaging  
 Multi-detector operation, laser multiplexing operation  
 cycle and repeat function, autosave function

Max. Image size, pixels (SPCM 64 bit software)	2048x2048	1024x1024	512x512
No of time channels, see [21]	256	1024	4096

### Data Acquisition Software, please see [21] for details

Operating system  
 Loading of system configuration  
 Start / stop of measurement  
 Online calculation and display, FLIM, PLIM  
 Online calculation and display, FCS, PCH  
 Number of images displayed simultaneously  
 Number of curves (Decay, FCS, PCH, Multiscaler)  
 Cycle, repeat, autosave functions

Windows 7 or Windows 8, 64 bit  
 single click in predefined setup panel  
 by operator or by timer, starts with start of scan, stops with end of frame  
 in intervals of Display Time, min. 1 second  
 in intervals of Display Time, min. 1 second  
 max 8  
 8 in one curve window  
 user-defined, used for  
 for time-series recording, Z stack FLIM,  
 microscope-controlled time series  
 User command or autosave function  
 Optional saving of parameter-tagged single-photon data  
 automatically after end of measurement or by user command

Saving of measurement data

Link to SPCImage data analysis



## References

1. E. Baggaley, S. W. Botchway, J. W. Haycock, H. Morris, I. V. Sazanovich, J. A. G. Williams, J. A. Weinstein, Long-lived metal complexes open up microsecond lifetime imaging microscopy under multiphoton excitation: from FLIM to PLIM and beyond. *Chem. Sci.* 5, 879-886 (2014)
2. E. Baggaley, M. R. Gill, N. H. Green, D. Turton, I. V. Sazanovich, S. W. Botchway, C. Smythe, J. W. Haycock, J. A. Weinstein, J. A. Thomas, Dinuclear Ruthenium(II) Complexes as Two-Photon, Time-Resolved Emission Microscopy Probes for Cellular DNA. *Angew. Chem. Int. Ed. Engl.* 53, 3367-3371 (2014)
3. Becker & Hickl GmbH, DCS-120 Confocal Scanning FLIM Systems, user handbook, edition 2012. [www.becker-hickl.com](http://www.becker-hickl.com), printed copies available
4. Becker & Hickl GmbH, The HPM-100-40 hybrid detector. Application note, available on [www.becker-hickl.com](http://www.becker-hickl.com)
5. Becker & Hickl GmbH, Spatially resolved recording of fluorescence-lifetime transients by line-scanning TCSPC. Application note, available on [www.becker-hickl.com](http://www.becker-hickl.com)
6. Becker & Hickl GmbH, DCS-120 Confocal Scanning FLIM System: Two-Photon Excitation with Non-Descanned Detection. Application note, available on [www.becker-hickl.com](http://www.becker-hickl.com)
7. Becker & Hickl GmbH, DCS-120 Confocal FLIM system with wideband beamsplitter. Application note, available on [www.becker-hickl.com](http://www.becker-hickl.com)
8. Becker & Hickl GmbH, Non-Descanned FLIM Detection in Multiphoton Microscopes. Application note, available on [www.becker-hickl.com](http://www.becker-hickl.com)
9. Becker & Hickl GmbH, Megapixel FLIM with bh TCSPC Modules - The New SPCM 64-bit Software. Application note, available on [www.becker-hickl.com](http://www.becker-hickl.com)
10. Becker & Hickl GmbH, TCSPC at Wavelengths from 900 nm to 1700 nm. Application note, available on [www.becker-hickl.com](http://www.becker-hickl.com)
11. Becker & Hickl GmbH, Modular FLIM systems for Zeiss LSM 510 and LSM 710 family laser scanning microscopes. User handbook. Available on [www.becker-hickl.com](http://www.becker-hickl.com)
12. Becker & Hickl GmbH, Burst Analyser 2.0, for correlation analysis and single-molecule spectroscopy. Available on [www.becker-hickl.com](http://www.becker-hickl.com)
13. W. Becker, A. Bergmann, C. Biskup, T. Zimmer, N. Klöcker, K. Benndorf, Multi-wavelength TCSPC lifetime imaging, *Proc. SPIE* 4620 79-84 (2002)
14. W. Becker, A. Bergmann, M.A. Hink, K. König, K. Benndorf, C. Biskup, Fluorescence lifetime imaging by time-correlated single photon counting, *Micr. Res. Techn.* 63, 58-66 (2004)
15. W. Becker, *Advanced time-correlated single-photon counting techniques*. Springer, Berlin, Heidelberg, New York, 2005
16. W. Becker, A. Bergmann, C. Biskup, Multi-Spectral Fluorescence Lifetime Imaging by TCSPC, *Micr. Res. Techn.* 70, 403-409 (2007)
17. W. Becker, B. Su, K. Weisshart, O. Holub, FLIM and FCS Detection in Laser-Scanning Microscopes: Increased Efficiency by GaAsP Hybrid Detectors. *Micr. Res. Techn.* 74, 804-811 (2011)
18. W. Becker, B. Su, A. Bergmann, K. Weisshart, O. Holub, Simultaneous Fluorescence and Phosphorescence Lifetime Imaging. *Proc. SPIE* 7903, 790320 (2011)
19. W. Becker, *Fluorescence Lifetime Imaging - Techniques and Applications*. *J. Microsc.* 247 (2) (2012)
20. W. Becker, V. Shcheslavskiy, FLIM with near-infrared dyes. *Proc. SPIE* 8588 (2013)
21. W. Becker, *The bh TCSPC handbook*. 6th edition. Becker & Hickl GmbH (2014), [www.becker-hickl.com](http://www.becker-hickl.com), printed copies available
22. W. Becker, V. Shcheslavskiy, S. Frere, I. Slutsky, Spatially Resolved Recording of Transient Fluorescence-Lifetime Effects by Line-Scanning TCSPC. *Microsc. Res. Techn.* 77, 216-224 (2014)
23. W. Becker, *Introduction to Multi-Dimensional TCSPC*. In W. Becker (ed.) *Advanced time-correlated single photon counting applications*. Springer, Berlin, Heidelberg, New York (2015)
24. W. Becker, V. Shcheslavskiy, H. Studier, TCSPC FLIM with Different Optical Scanning Techniques, in W. Becker (ed.) *Advanced time-correlated single photon counting applications*. Springer, Berlin, Heidelberg, New York (2015)
25. M. Y. Berezin, S. Achilefu, Fluorescence lifetime measurement and biological imaging. *Chem. Rev.* 110(5), 2641-2684 (2010)
26. B. Chance, B. Schoener, R. Oshino, F. Itshak, Y. Nakase, Oxidation-reduction ratio studies of mitochondria in freeze-trapped samples. NADH and flavoprotein fluorescence signals *J. Biol. Chem.* 254, 4764-4771 (1979)
27. D. Chorvat, A. Chorvatova, Multi-wavelength fluorescence lifetime spectroscopy: a new approach to the study of endogenous fluorescence in living cells and tissues. *Laser Phys. Lett.* 6 175-193 (2009)
28. M.A. Digman, V.R. Caiofla, M. Zamai, E. Gratton, The phasor approach to lifetime imaging analysis. *Biophys. J.* 94, L16-L17
29. R. I. Dmitriev, A. V. Zhdanov, Y. M. Nolan, D. B. Papkovsky, Imaging of neurosphere oxygenation with phosphorescent probes. *Biomaterials* 34, 9307-9317 (2013)

30. R. I. Dmitriev, A. V. Kondrashina, K. Koren, I. Klimant, A. V. Zhdanov, J. M. P. Pagan, K. W. McDermott, D. B. Papkovsky, Small molecule phosphorescent probes for O<sub>2</sub> imaging in 3D tissue models. *Biomater. Sci.* 2, 853-866 (2014)
31. S. Felekyan, Software package for multiparameter fluorescence spectroscopy, full correlation and multiparameter imaging. Available from [www.mpc.uni-duesseldorf.de/seidel/software.htm](http://www.mpc.uni-duesseldorf.de/seidel/software.htm)
32. Th. Förster, Zwischenmolekulare Energiewanderung und Fluoreszenz, *Ann. Phys. (Serie 6)* 2, 55-75 (1948)
33. S. Frere, I. Slutsky, Calcium imaging using Transient Fluorescence-Lifetime Imaging by Line-Scanning TCSPC. In: W. Becker (ed.) *Advanced time-correlated single photon counting applications*. Springer, Berlin, Heidelberg, New York (2015)
34. V. Katsoulidou, A. Bergmann, W. Becker, How fast can TCSPC FLIM be made? *Proc. SPIE* 6771, 67710B-1 to 67710B-7
35. J. Jenkins, R. I. Dmitriev, D. B. Papkovsky, Imaging Cell and Tissue O<sub>2</sub> by TCSPC-PLIM. In: W. Becker (ed.) *Advanced time-correlated single photon counting applications*. Springer, Berlin, Heidelberg, New York (2015)
36. J.R. Lakowicz, *Principles of Fluorescence Spectroscopy*, 3rd edn., Springer (2006)
37. D. B. Papkovsky, and R. I. Dmitriev, Biological detection by optical oxygen sensing, *Chem Soc Rev* 42, 8700-8732 (2013)
38. R. Richards-Kortum, R. Drezek, K. Sokolov, I. Pavlova, M. Follen, Survey of endogenous biological fluorophores. In M.-A. Mycek, B.W. Pogue (eds.), *Handbook of Biomedical Fluorescence*, Marcel Dekker Inc. New York, Basel, 237-264 (2003)
39. M. C. Skala, K. M. Ricking, D. K. Bird, A. Dendron-Fitzpatrick, J. Eickhoff, K. W. Eliceiri, P. J. Keely, N. Ramanujam, In vivo multiphoton fluorescence lifetime imaging of protein-bound and free nicotinamide adenine dinucleotide in normal and precancerous epithelia. *J. Biomed. Opt.* 12 02401-1 to 10 (2007)
40. H. Studier, W. Becker, Megapixel FLIM. *Proc. SPIE* 8948 (2014)
41. C. Toncelli, O. V. Arzhakova, A. Dolgova, A. L. Volynskii, N. F. Bakeev, J. P. Kerry, D. B. Papkovsky, Oxygen-sensitive phosphorescent nanomaterials produced from high density polyethylene films by local solvent-crazing. *Anal. Chem.* 86(3), 1917-23 (2014)
42. S. Weidkamp-Peters, S. Felekyan, A. Bleckmann, R. Simon, W. Becker, R. Kühnemuth, C.A.M. Seidel. Multiparameter fluorescence image spectroscopy to study molecular interactions. *Photochem. Photobiol. Sci.* 8, 470-480 (2009)







**Becker & Hickl GmbH**

Nahmitzer Damm 30

12277 Berlin, Berlin

Tel. +49 / 30 / 787 56 32, Fax. +49 / 30 / 787 57 34

email: [info@becker-hickl.com](mailto:info@becker-hickl.com), [www.becker-hickl.com](http://www.becker-hickl.com)